

AN ABSTRACT OF THE THESIS OF

Yong J. Li for the degree of Master of Science in Chemical Engineering presented on March 5, 2012.

Title: Continuous Synthesis of Metal-organic Frameworks Under High Pressure

Abstract approved:

Kenneth J. Williamson

Metal Organic Framework (MOF) materials, consisting of metal ions with organic linkers, have a functional cavity structure which can be utilized in applications such as catalyst, micro sensing, and gas absorption. Due to MOF materials' selective gas adsorption property, interest in MOF materials has intensified in the last few years, particularly for CO, CO₂, N₂, CH₄, and H₂. MOF materials are typically synthesized by reaction under hydrothermal conditions which yields a highly crystalline product. However, reaction under solvothermal condition typically requires long reaction times - from 8 hours up to several days depending upon the particular MOF material and the reaction conditions, such as solvent, temperature, and concentration. Other synthesis methods that have been developed to address these issues include microwave synthesis, sonochemical synthesis, and mechanochemical synthesis. Reaction time can be reduced to minutes under the high energy conditions of a microwave synthesis method. A solvent free synthesis can be achieved using the mechanochemical synthesis. The sonochemical synthesis method provides an environmentally friendly process.

However, all of these synthesis methods above are batch processes and meet several difficulties in scalability and controllability. Herein, we introduce a new synthesis method for MOF materials which utilizes a continuous flow reactor process. To reduce the reaction time and solvent usage, and to maintain a high degree of the crystallinity are the goals of this study. Cu-BTC (BTC = Benzene, -1,3,5-Tricarboxylate) or HKUST-1 Metal Organic Framework material was chosen to demonstrate the continuous flow reactor process since it has a simple MOF structure, consisting of Cu^{+2} ions and BTC linkers, and has been widely studied for catalyst applications. The continuous flow synthesis method shows successful results of reduced residence time as low as 5 minutes, high crystal quality obtained, size control, and high yield with recycle solvent cooperation. The particle size control of MOF material has been shown crucial contributions in absorption application and is accomplished by adjusting the system temperature, flow rate, and solvent composition ratio. A water/ethanol mixture as the solvent in Cu-BTC synthesis reaction is environmentally friendly and easy to separate from the MOF product. In addition, the composition of water in solvent is the most influential factor to the crystal growth rate specifically in crystallization rate and nucleation rate. BTC is used in excess to achieve a production yield of about 97% based on Cu ion consumption. Since the Cu-BTC particles have a low solubility in the ethanol/water solution, they can be obtained easily using a dispersion/sonication method. The BTC rich supernatant can be recycled for use in the feed stream to maintain a high production rate, which can be beneficial for quick economic production in laboratory, as well as, commercial scale applications.

©Copyright by Yong J. Li

March 5, 2012

All Rights Reserved

Continuous Synthesis of Metal-organic Frameworks
Under High Pressure

by
Yong J. Li

A THESIS

submitted to

Oregon State University

in partial fulfillment of
the requirements for the
degree of

Master of Science

Presented March 5, 2012
Commencement June 2012

Master of Science thesis of Yong J. Li presented on March 5,2012.

APPROVED:

Major Professor, representing Chemical Engineering

Head of the School of Chemical, Biological & Environmental Engineering

Dean of the Graduate School

I understand that my thesis will become part of the permanent collection of Oregon State University libraries. My signature below authorizes release of my thesis to any reader upon request.

Yong J. Li, Author

ACKNOWLEDGEMENTS

I would like to express my gratitude to my advisor, Dr. Kenneth J. Williamson, who provided a great opportunity for me to perform a professional study and research. I appreciate that Dr. Chih-hung Chang assigned a challenging project to me and guided me into a professional thinking.

I would like to thank the technical support from Chemical Engineering technical support team Andrew Brickman who provided system development experience and provide suggestions on component selection. I would also like to thank Manfred Dittrich who assisted in manufacturing custom made components.

I would like to thanks my lab mates, Wei Wang, Yu-Wei Su, Chang-Qing Pan, Chang-Ho Choi, Kathy Han, Toey Paravee, Mike Knapp, Peter Kreider, Dr. Seung-Yeol Han, and Dr. Ki-Joong Kim.

I would like to thank the help from OSU Electron Microscopy and Imaging Facility. Director, Dr. Yi Liu, and Senior Faculty Research Assistant, Teresa Sawyer, provided essential assistance and expertise in capturing high quality images to support my research.

Finally, I would like to thank my wife, my son, and my parents who support my research work. Thank you.

TABLE OF CONTENTS

	<u>Page</u>
1 Introduction.....	1
2 Background.....	3
2.1 Metal Organic Framework (MOF).....	3
2.2 Porous structure	6
2.3 Cu-BTC crystal structure	6
2.4 Crystallization grow rate and nucleation grow rate.....	8
2.5 Application of MOF.....	9
2.6 Synthesis methods.....	13
2.7 Film deposition methods.....	17
3 Design of system and experiment.....	18
3.1 Design of experiment loop.....	18
3.2 Heat exchange unit.....	19
3.3 Condenser design.....	22
3.4 Overall system design.....	23
3.5 First version of system.....	24

TABLE OF CONTENTS (Continued)

	<u>Page</u>
3.6 Experimental design.....	27
3.7 System upgrade version.....	29
4 Results and discussions.....	31
4.1 X-ray Diffraction (XRD).....	31
4.2 Raman characterization.....	32
4.3 SEM image.....	33
4.4 Water effect.....	36
4.5 Stoichiometry ratio effect.....	38
4.6 Temperature effect.....	41
4.7 Film deposition.....	43
5 Conclusion and future work.....	46
Bibliography.....	48
Appendix A.....	50

LIST OF FIGURES

	<u>Page</u>
2.1.1 Classes of MOFs coordination polymers based on topology networks	4
2.1.2 Examples of linkers used in coordination polymers.....	5
2.2 Single-crystal x-ray structures of MOF-5. Zn, blue polyhedron; O, red spheres; C, black spheres, hydrogen atoms have been omitted.....	6
2.3 The structure of the MOF Cu-BTC	7
2.5.1 Binary mixture gas go through a MOF material layer.....	11
2.5.2 Snapshots of the structures of Cu-BTC with adsorbed binary mixture of CO ₂ /N ₂ with gas composition CO ₂ :N ₂ =15.6:84.4 at three pressures: (a) P=0.1 MPa, (b) P=1.0 MPa, (c) P=5.0 MPa.....	12
2.6 Schematic of Solvothermal reactions.....	13
2.8 Schematic diagram of the layer-by-layer growth of the metal-organic polymer on the MHDA SAM obtained by repeated immersion cycles for 60 min in solutions of Zn(CH ₃ CO ₂) ₂ , (Zn(OAc) ₂), and then BTC.....	17
3.1 Flowchart of Design of Experiment (DoE).....	18
3.2 Schematic of heating zone, reaction zone, and cooling zone design....	20
3.4 Schematic of first version of overall continuous flow reaction system design	24
3.5 Picture of the first version of the synthesis system.....	26
3.7 Picture of the upgraded version of the synthesis system.....	30

LIST OF FIGURES (Continued)

	<u>Page</u>
4.1 XRD patterns of Cu-BTC samples of (a) batch reaction method and (b) continuous reaction method. Reflections for Cu-BTC calculated from the crystal structure are given for comparison.....	32
4.2 Raman Spectra of batch and continuous reaction samples.....	33
4.3 SEM image of Cu-BTC samples of (a) Solvothermal batch reaction (b) continuous reaction.....	35
4.4 SEM image of Cu-BTC sample of (a) continuous reaction, (b) batch Reaction.....	37
4.5 XRD results of Cu-BTC crystal from (a) batch reaction, and from continuous flow reaction with Cu:BTC ratio in (b) 1:1, (c) 2:1, and (d) 1:3.....	40
4.6 SEM image of Cu-BTC with synthesis temperature at (a) 120 °C, (b) 65 °C.....	42
4.7.1 SEM image of Cu-BTC with synthesis temperature at 65 °C.....	44
4.7.2 SEM image of Cu-BTC deposited on the top of (a) (PAH/PSS)nPAH layer at n=5, (b) (PAH/PSS)nPAH layer n=7, and (c) (PAH/PSS)n layer at n=5.....	45

LIST OF TABLES

	<u>Page</u>
2.1 The six basic hydrogen storage methods. The gravimetric density ρ_m , the volumetric density ρ_v , the working temperature T and pressure p are listed. RT stands for room temperature.....	10
2.2 The yield of different synthesis methods for Cu-BTC material.....	16
3.1 List of experiment parameters and their level.....	27
4.1 Crystal growth at same reaction temperature, flow rate, pressure, and reactant ratio.....	38

Continuous Synthesis of Metal-organic Frameworks Under High Pressure

CHAPTER 1

Introduction

Energy crisis due to the limitation of fossil oil resources will be a serious problem for our generation. Many researchers are looking for renewable energy such as wind, solar, geothermal, and hydropower. Saving energy or increasing the efficiency of the energy usage is a very hot topic. Hydrogen is a great energy carrier and can be directly used as the fuel since it has high energy content, three times the energy per pound of gasoline and produces a clean exhaust product water vapor without carbon dioxide. [1] The biggest disadvantage besides problems with safety is that the density of compressed hydrogen in gas form is just one tenth compared to gasoline, which means a huge storage container is needed to provide the same amount of energy. The most common hydrogen storage method is to use a metal cylindrical vessel to store compressed hydrogen. Cryogenic liquid, adsorption to high surface-area materials, and chemical storage as metal hydrides are other options for hydrogen storage. Adsorption to high surface-area materials like metal-organic framework (MOF) has attracted great attention in the last decade.[2] This method is only based on the physisorption, which means no reaction is involved. Adsorption of hydrogen gas would increase proportional to reduced system temperature and to increased system pressure. A great potential application may be in the automobile industry with hydrogen-powered vehicles. The following chapter will introduce hydrogen adsorption and synthesis of MOF material.

MOF materials can also be used to combat the problem of greenhouse gas emissions by applying their enhanced adsorption abilities.[3, 4] Researchers from Li et al. found that MOF materials are great candidates to filter out the carbon dioxide on board internal combustion vehicles. [4] The CO₂-saturated MOF materials can periodically undergo a desorption process to remove the adsorbed CO₂ and can then be reused as a filter. This application has huge potential for the future.

The size of the MOF material is important in some research areas such as microsensors, microfilters, and catalysts. The common crystal size of MOF materials is about one micron in diameter. Researchers are very interested to see if nanoscale MOF crystals behave the same as the larger size ones. MOF is a new type of porous material with a high surface area. There are thousands of potential MOF material combinations based on hundreds different organic linkers and metal ions. This gives great selection opportunities for the different pore sizes and chemical properties. Our study started with a very simple and common MOF of Cu and BTC framework. We show that fast grown, nanoscale Cu-BTC crystals can be produced by a continuous flow reaction synthesis under high pressure.

Chapter 2

Background

2.1 Metal Organic Framework (MOF)

A porous material which consists of linker and connector are recognized as coordination polymer around 1960 and first reported by Tomic[5]. The metal ions as the center connector are usually chosen from Cu, Zn, Mn, and Co. The coordination polymer is a new class of porous material to the two traditional type of porous material, inorganic and carbon based materials. The connectors-linkers building blocks form continuous porous network structures that can be classified by porous structure as dots (0D cavity), channels (1D space), layers (2D space), and intersecting channels (3D space). Based on the porous structure, the application of the coordination polymer can be applied to separation, storage, and heterogeneous catalysis due to the interest in the creation of nanometer-sized spaces and the novel phenomena in the porous compounds. However, a more general term Metal-Organic Frameworks was introduced, and has attracted great attention after the group of O.M. Yaghi published a simulation on MOF-5 structure in 1995.[6] Metal Organic Frameworks (MOF) are crystalline compounds consisting of metal ions or clusters coordinated to often rigid organic molecules to form a continuous one, two, or three dimensional network. Due to the high surface area and controllable porous structure property, MOF became a great candidate for adsorption applications. There is no difference of definition between coordination polymer and metal organic framework in scientific literature, but the term MOF becomes more popular in last

decade since it shows a great potential in catalysis, gas storage, gas separation, and micro sensing.

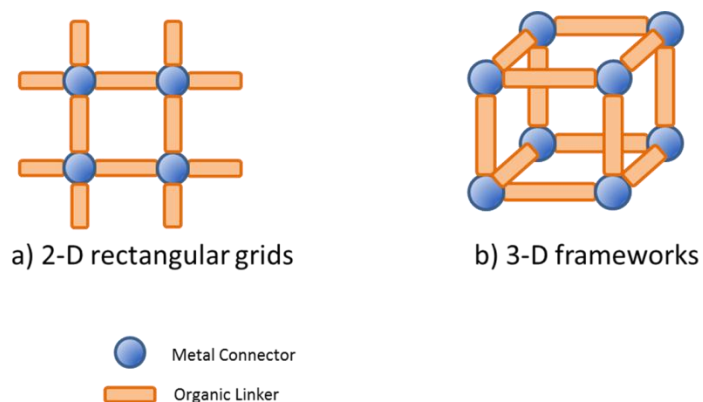


Figure 2.1.1 Classes of MOFs coordination polymers based on topology networks

These continuous building networks possess many cavities to create a high porous structure surface area where cavity diameter is dependent on the selection of organic linkers. The common organic linkers are shown in **Figure 2.1.2**. The number of combination of MOFs is up to hundreds of thousands and is the product of metal ions and organic linkers.

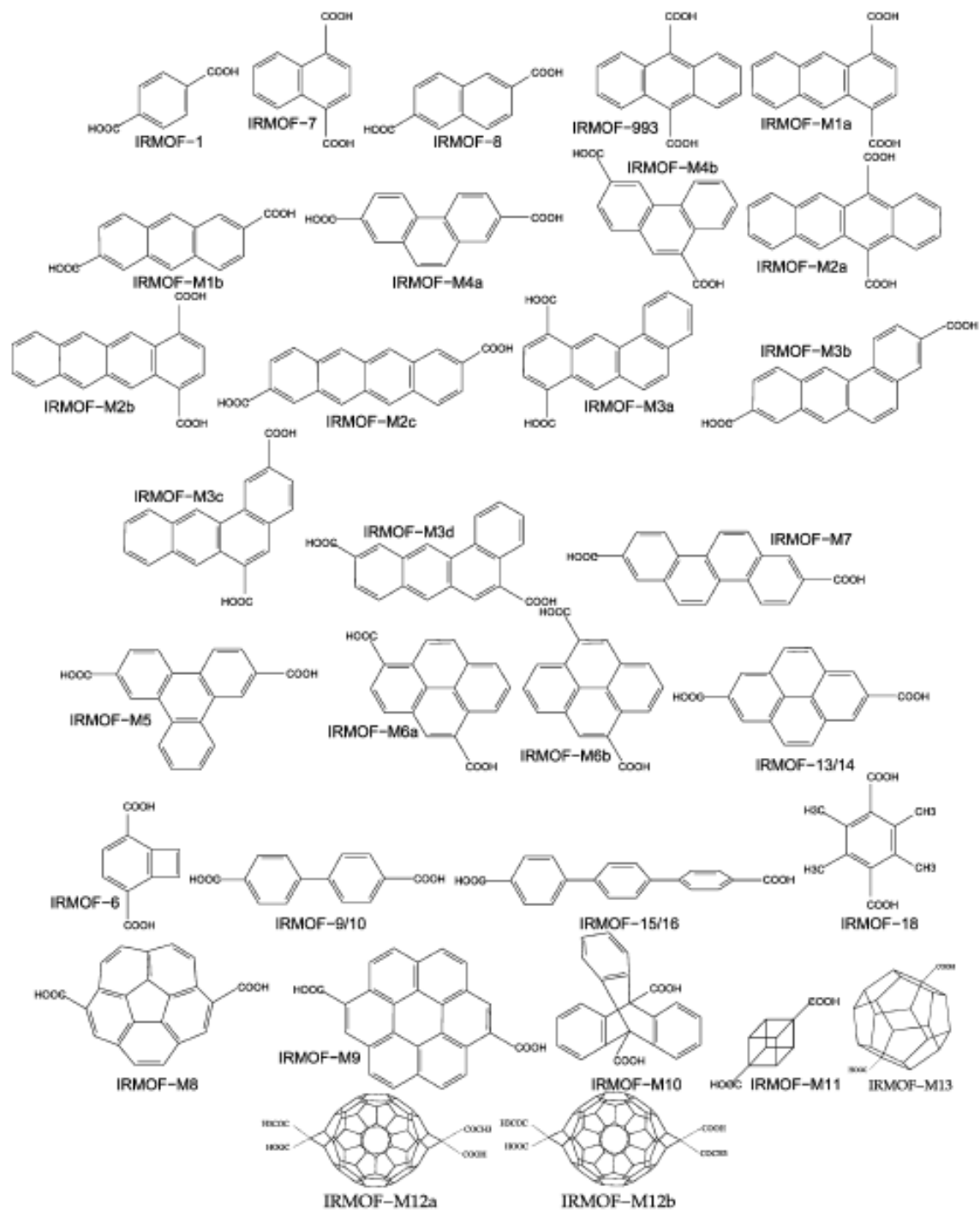


Figure 2.1.2 Examples of linkers used in coordination polymers. [7]

2.2 Porous structure

Homogeneous periodic pores of MOF material are tunable varied from 3.8 to 28.8 angstroms with an open space represented up to 91.1% of the crystal volume.[8]

Octahedral $\text{Zn}_4\text{O}(\text{CO}_2)_6$ clusters and varying dicarboxylate organic linkers demonstrate different MOF combinations with different cavity capacity and functional property as shown in **Figure 2.2** with a single cube fragment of their respective cubic three-dimensional extended structure. The cluster $\text{Zn}_4\text{O}(\text{CO}_2)_4$ of an oxygen-centered Zn_4 tetrahedron bridges six carboxylate organic linkers to form a corner of cubic MOF building block. The large yellow spheres represent the maximum internal space that would fit in the cavities without touching the van der Waals atoms of the frameworks.

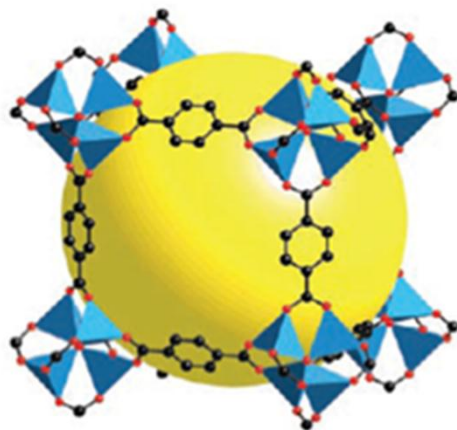


Figure 2.2 Single-crystal x-ray structures of MOF-5. Zn, blue polyhedron; O, red spheres; C, black spheres, hydrogen atoms have been omitted. [8]

2.3 Cu-BTC crystal structure

Cu-BTC, one of the most common MOFs materials that has a single benzene ring with a carboxylic group and copper ions, was chosen to apply the continuous reactor for scale

up processing. Two copper ions form a Cu-Cu bond at the center of the cluster and connect four pairs of carboxylates to build a three dimensional open network. The diameter of the cavity is about 12 angstroms. [9]

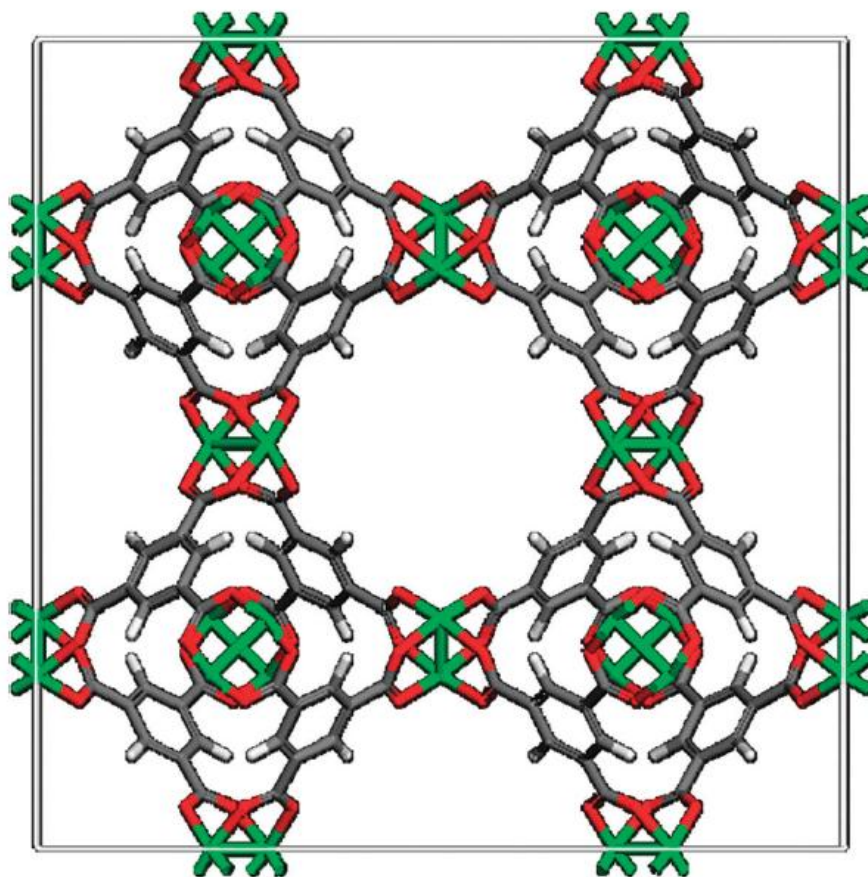
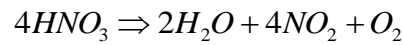
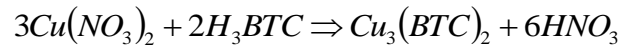


Figure 2.3 The structure of the MOF Cu-BTC (green: copper; red: oxygen; black; carbon; white: hydrogen).[9]

Chemical reaction of the Cu-BTC synthesis is completed by mixing copper nitrate solution with trimesic acid solution. A porous crystalline Cu-BTC is the product and nitric acid is the byproduct from the chemical reaction. The nitric acid decomposes into nitrogen dioxide, water, and oxygen. The most common synthesis method is solvothermal reaction where reaction is hold under a hydrothermal condition, which will be introduced in the chapter 3.



2.4 Crystallization growth rate and nucleation grow rate

The growth of the metal-organic framework (MOF) materials is dependent on the crystallization growth rate and nucleation growth rate, since they are crystalline compounds.[10] For example, Cu-BTC crystal with hydrothermal synthesis method is produced by mixing metal ionic precursor and organic linker precursor. The nucleation growth rate can be estimated with the equation below,

$$J_N = B_N \exp\left(-\frac{\Delta G^N}{RT}\right)$$

$$\Delta G^N = \frac{16\pi\gamma^3 V_m^2}{3|\Delta\mu|^2}$$

where J_N is crystal nucleation rate per unit volume, ΔG^N is activation energy for homogeneous nucleation, γ is surface tension, V_m is molar volume of solid, $\Delta\mu$ is difference in chemical potential between solid and monomers, and B_N is the pre-exponential factor depending on many parameters such as desolvation of species. The crystallization grow rate can be estimated as temperature dependent by using the theory of Arrhenius equation.

2.5 Application of MOF

Two major applications of MOF are gas storage and separation. Hydrogen is the most abundant energy carrier on the earth. It is a challenge to store the hydrogen since its critical point is as low as 32.97K at 1.293MPa. The most common hydrogen storage method is high-pressure gas cylinders with a maximum pressure of 200 bar. There is a tradeoff between the wall thickness of the cylinder and the maximum pressure of the gas to gain a larger volumetric density. Therefore, recent research reported to achieve high pressure as 800 bar with a light weight material gas cylinders. Other storage methods are liquid hydrogen in cryogenic tanks, absorbed on interstitial sites in a host metal such as group one, two and three light weight metal, chemically bonded in covalent and ionic compounds through oxidation of reactive metals with water and adsorbed hydrogen on materials with a large specific surface area are the other major hydrogen storage methods.

Table 2.1 The six basic hydrogen storage methods. The gravimetric density ρ_m , the volumetric density ρ_v , the working temperature T and pressure p are listed. RT stands for room temperature. [11]

Storage method	ρ_m (mass%)	ρ_v (kg H ₂ m ⁻³)	T(°C)	p (bar)
High-pressure gas cylinders	13	<40	RT	800
Liquid hydrogen in cryogenic tanks	Size dependent	70.8	-252	1
Adsorbed hydrogen	≈ 2	20	-80	100
Absorbed on interstitial sites in a host metal	≈ 2	150	RT	1
Complex compounds	<18	150	>100	1
Metals and complexes together with water	<40	>150	RT	1

The surface area of the MOFs material, depending on the linker size and functional linker group, can extend up to $6000\text{m}^2/\text{g}$. [12] MOF material consists of continuous porous structure which contains many small cavities to adsorb selectively of particles such as small atoms or molecules. With increasing surface area, a diffusion dominated permeation mechanism was proved from the molecule size changing from small to large, such as $\text{H}_2 > \text{He} > \text{CO} > \text{N}_2 > \text{CO}_2 > \text{SF}_6$. [13]

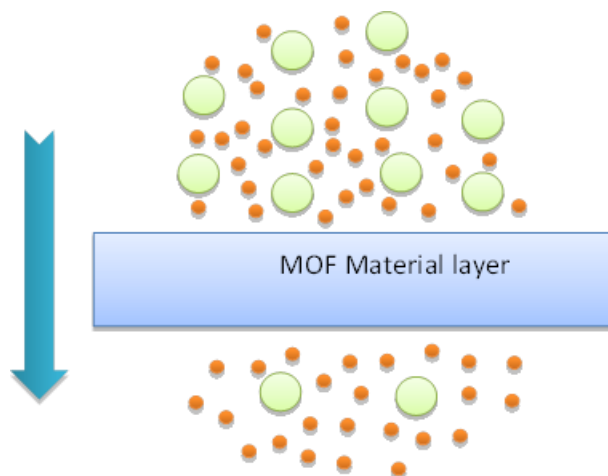


Figure 2.5.1 A binary mixture gas go through a MOF material layer.

A simulation structure study of MOF by Yang *et. al.* used Materials Visualizer based on the experimental XRD data. [14] A selectivity of adsorption for Cu-BTC is shows in **Figure 2.5.2** under different pressure. A binary gas mixture ratio of CO_2/N_2 of 15.6:84.4 is adsorbed by Cu-BTC material under different pressures as 1, 10, and 50 Bar. Yang *et. al.* found that CO_2 was preferentially adsorbed by Cu-BTC under these conditions and that the effect remained at even higher pressures.

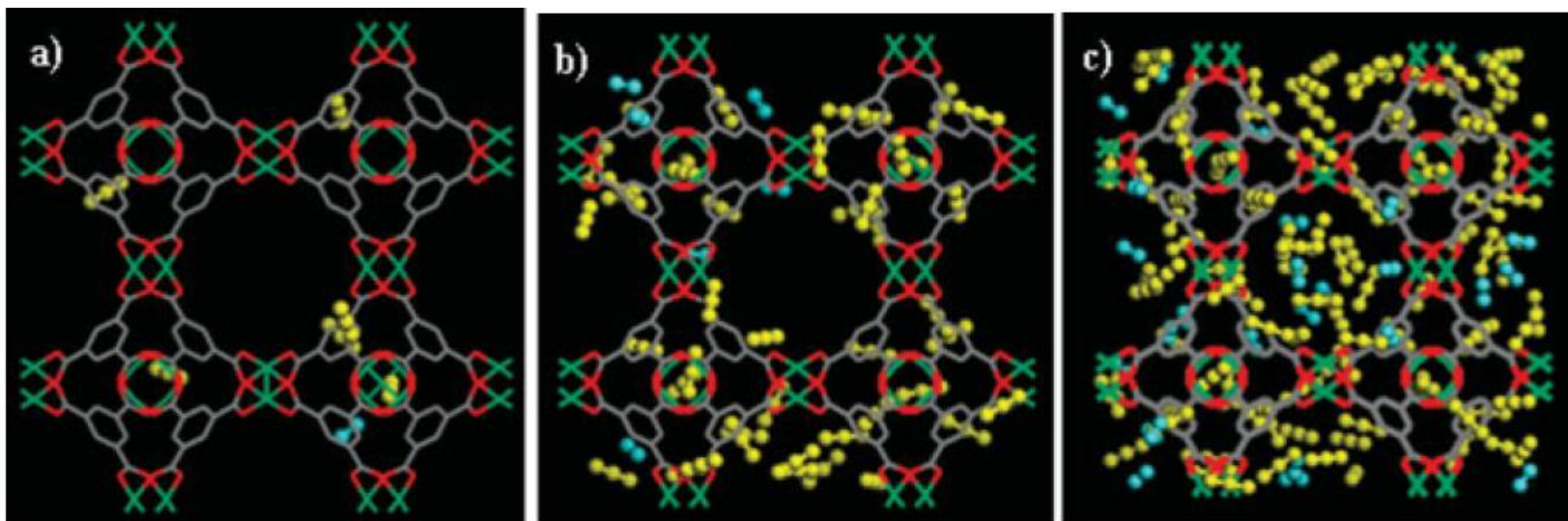


Figure 2.5.2. Snapshots of the structures of Cu-BTC with adsorbed binary mixture of CO₂/N₂ with gas composition CO₂:N₂=15.6:84.4 at three pressures: (a) P=0.1 MPa, (b) P=1.0 MPa, (c) P=5.0 MPa. (Cu-BTC framework is shown in line style with atoms H omitted for clarity; CO₂, yellow ball-stick style; N₂, green ball-stick style). [14]

2.6 synthesis methods

2.6.1 Solvothermal Reaction

Solvothermal reaction is the most common synthesis method to produce MOF material.

A hydrothermal reactor is used which consists of a special stainless steel autoclave with a Teflon internal cup. Two different precursors are prepared individually and are mixed into the reaction vessel. The mixture needs to be well mixed for at least 10 minutes.

The vessel is closed and placed into a furnace for 18 to 24 hours at desired reaction temperatures.[15] After reaction time is completed, decrease the temperature to room temperature and collect MOF particles by separating the liquid solution from the particle. The liquid solution contains the left over precursors and byproducts. For particles, perform a three cycle centrifugal and disperse process. Finally, ultrapure MOF crystal can be achieved.

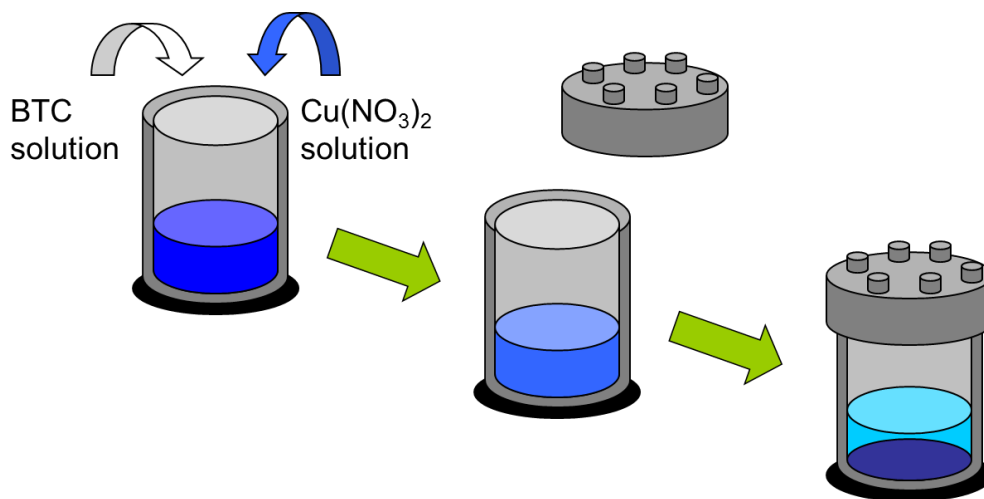


Figure 2.6 Schematic of Solvothermal reactions

2.6.2 Reflux synthesis method

Solvothermal reaction method can provide a higher reaction temperature to allow crystal grow gradually to achieve more uniformly. It is required to use an autoclave to maintain a pressurized condition to enhance a homogeneous reaction. The drawback of the autoclave is not easy to sample without releasing pressure which drop the solution temperature. To apply a reflux synthesis method, a condenser-three neck flask design would be an easy way to test the reaction mechanism while maintaining ambient conditions.

The reflux system is consisted of a three neck flask, condenser, heating bath, stir function build-in hot plate, k-type thermal couple, and PID temperature controller. The two different precursors were poured into the three neck flask and mixed by a magnetic stir bar. A k-type thermal couple was placed into the flask to read the temperature from the mixture solution. The PID temperature controller is used to receive the temperature signal and provide the thermal energy to the bottom of the flask as the feedback controller. The maximum reaction temperature would be limited by the exact boiling point of the solvent. The reaction can be run as long as needed since the reactant solvent would not escape from the system.

2.6.3 Other synthesis methods

In order to achieve higher purity and crystallinity of the products in a shorter reaction time, many other synthesis methods are developed and have been reported, such as microwave-assisted synthesis and mechanochemical synthesis.

The microwave-assisted hydrothermal synthesis provides a fast heating, quick kinetics, phase purity, high yield and good reliability and reproducibility compare with conventional hydrothermal synthesis method. A typical process is to start with mixed precursors and then placed into a microwave reactor. The reaction time is related to the reaction temperature which is also in term of the microwave power. The reaction setting can be 5 to 20 minutes and 120 °C to 180°C[16]. Recent research also found that the nucleation rate of the reaction is enhanced rather than the crystallization rate which can explain why the microwave-assisted method can reduce the reaction time from 18 hours down to 30 minutes. Yoo's research group combined microwave and conventional hydrothermal method which can balance both nucleation and crystallization rate. A major drawback to this method is the size of the equipment and the requirement for a batch reaction process.

MOF material can be synthesized without solvents present such as applying mechanochemical method.[17] Ball Mills is the most common equipment unit to contain the solid reactant and allow a chemical reaction at solid phase. Two or more reactants in solid phase are mixed and then introduced into the ball mills to facilitate the reaction with the mechanical grinding motions. The production yield of this synthesis method can be over 97%, which is as good as solvothermal reaction and microwave-assisted methods. The applications of MOF material are most likely in solid phase without presence of solvent. Production cost can be reduced without a solvent separation process.

Table 2.2 The yield of different synthesis methods for Cu-BTC material. [11]

Synthesis method	Reaction time	Base	Yield
Solvothermal synthesis	24 hours	984mg Copper (II) acetate	93%
Reflux synthesis under ambient pressure	6 hours	600mg Copper (II) acetate	87%
Ultrasonic irradiation synthesis	1 hour	200mg Copper (II) acetate	71%
Electrochemical synthesis	30 min	981mg H ₃ BTC	49%
Mechanochemical synthesis	20 min	982mg Copper (II) acetate	97%
Microwave-assisted synthesis	5 min	177mg Copper (II) nitrate	96%

2.7 Film deposition methods

The most common application of MOF crystal is film deposition for micro or nanoscale applications. There are a few types of synthesis methods that have been developed in the past decade. One is the crystal growth on a self-assembled monolayer (SAM) layer. Another method is crystal growth on a metal oxide layer such as Al_2O_3 with solvothermal reaction. A common SAM layer contains a sixteen carbon chain, 16-mercaptohexadecanoic acid (MHDA), and is reacted with zinc to form Zn-BTC. The sulfur end of the MHDA anchors the material to the substrate and the carboxylic end connects to the BTC molecule. [19] First, the substrate is coated with a SAM layer and then it is dipped into a BTC solution and then into a Zinc acetate solution. Then the dipping process for BTC and zinc acetate solution is repeated alternatively. It takes 60 minutes in each solution, resulting in a days long deposition procedure. A uniform alternative layer of Zinc-BTC MOF structure is developed.

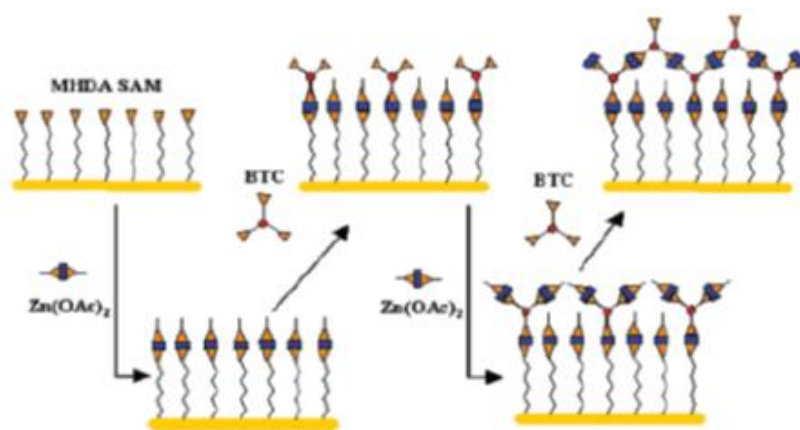


Figure 2.7.1 Schematic diagram of the layer-by-layer growth of the metal-organic polymer on the MHDA SAM obtained by repeated immersion cycles for 60 min in solutions of $\text{Zn}(\text{CH}_3\text{CO}_2)_2$, $\text{Zn}(\text{OAc})_2$, and then BTC. For simplicity, the scheme simplifies the assumed structural complexity of the carboxylic acid coordination modes. [18]

Chapter 3

Design of system and experiment

3.1 Design of experiment loop

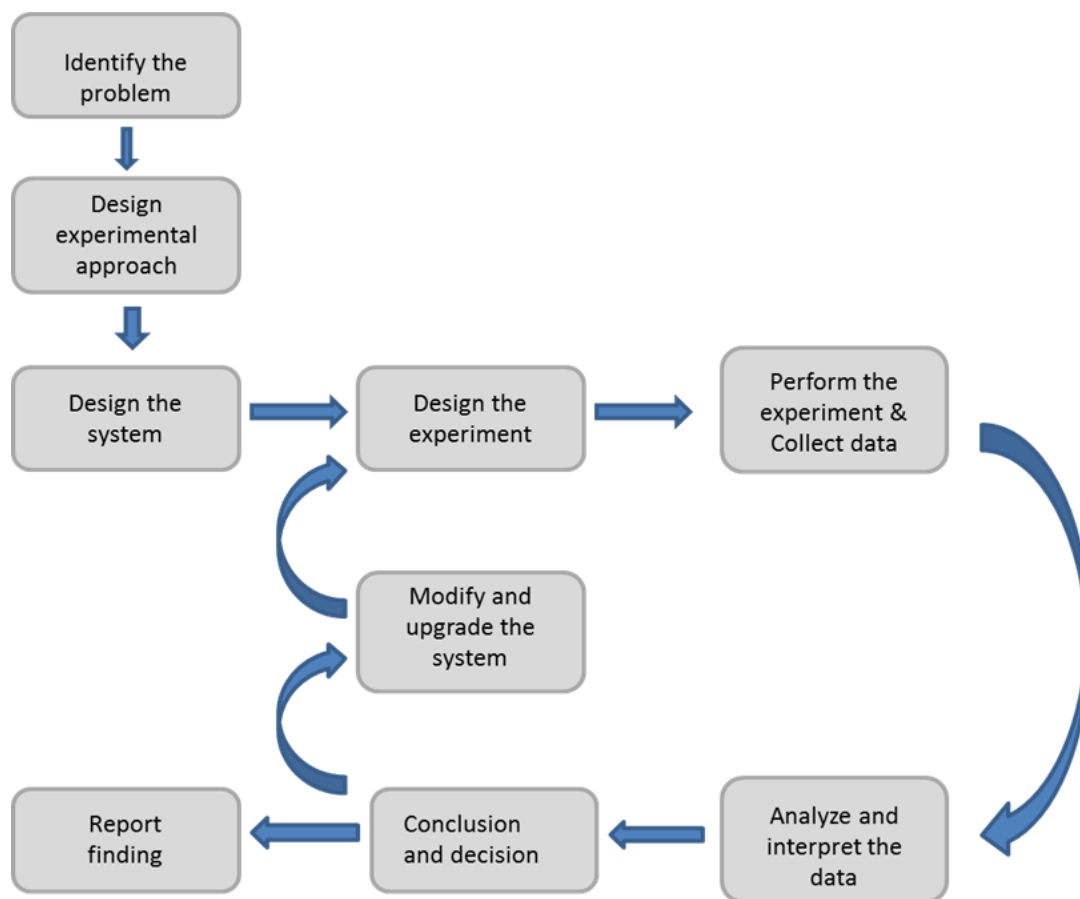


Figure 3.1 Flowchart of Design of Experiment (DoE)

This research started with a design diagram loop which applied the idea of Design of Experiment (DoE), shown in **Figure 3.1** to develop a synthesis method to speed up and scale up the production rate of the Metal-organic framework (MOF) material with a proper production rate control. The problem of the current synthesis method is the production rate of the MOF material is too slow and it is not easy to scale up due to the

equipment limitation. Identifying the problem was the first step of the project.

Comparing with other synthesis methods, such as solvothermal reaction, microwave assisted, and ultrasonic assisted, a continuous flow reaction synthesis method will be a perfect solution to match all these demands.

A continuous flow micro-reactor system was created to produce the MOF material.

Based on the process and product requirements, a system flow chart shown in **Figure 3.4** was made of specific components such as pumps, tubing, and more. Next step, parameters or factors which may influence the result of the chemical reaction, heat transfer, and mass transfer were identified, such as reaction temperature, fluid flow rate, system pressure, and reaction residence time. Design of Experiment (DoE) was used to set up an experiment plan based on high and low level of each parameter to find the most important variable and interaction between two variables. The experiment was then performed under different experimental settings. Samples were analyzed for their crystal structure, morphology, and chemical absorption properties. Statistical tools were applied to the results. Then, conclusion was made from the analysis to either report the results or upgrade the system and perform the experiment again analyze.

3.2 Heat exchange unit

Increasing the reaction temperature, results in a faster reaction rate. The reaction temperature is controlled by the heat exchange unit which consists of three zones: heating zone, reaction zone, and cooling zone. Thermal energy was transferred from the heating unit into the system to preheat the reactant mixture from room temperature up to the reaction temperature. The heated mixture solution would maintain a constant

temperature through the reaction zone. The duration of the chemical reaction depended on the residence time in terms of the flow rate and reaction zone length. The chemical reaction was then stopped by cooling down the reaction temperature by passing through the cooling zone. The cooling rate of the system would depend on the size of the cooling unit and the flow rate of the cooling fluid. A schematic of heat exchange unit is shown in **Figure 3.2**.

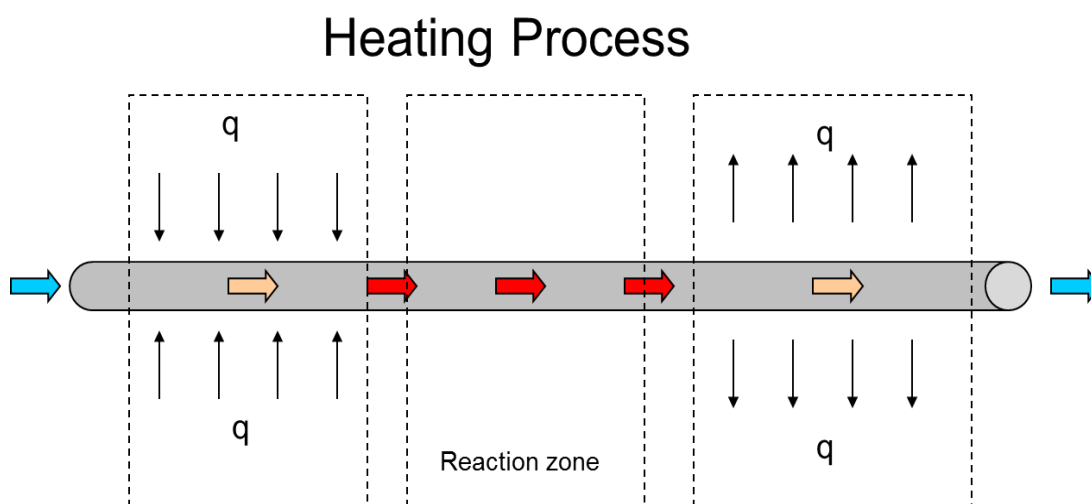


Figure 3.2 Schematic of heating zone, reaction zone and cooling zone design

The heating zone design can be chosen from several options such as oil bath heating assisted, electrical lamp assisted, electrical heating rope assisted, or a ceramic heating furnace. The biggest concern of the flow reactor is the safety issue. The continuous flow reaction is required high pressure to keep homogenous liquid-liquid reaction under a high reaction temperature, requiring extra attention to safety. An ideal heating method has to be easy to control especially to turn off or shut down quickly when the system experiences an unexpected situation such as leaking liquid, irregular pressure, or

accidental changes in temperature. An oil bath-assisted heating method can provide a constant heating flux in terms of uniform temperature profile but the response of the heating or cooling rate is very slow. Regarding safety, it may require a more complicate design to upgrade emergency stop function compared to other heating methods. A halogen lamp can provide constant radiation energy and transfer into thermal energy. It is clean and easy to control, but it requires a certain amount of system space especially for a multi-control heating zone design. Compared with other electrical heating methods, the electrical heating rope method has some key advantages that match the design requirements. First, the heating component can turn off immediately to avoid overheating. Second, due to the heat flux capacity limit, the heating rope could not provide an extreme high reaction temperature but it would be perfect for the MOF synthesis which maximum temperature will be less than 330°C to avoid damaging the crystal structure of the product. Third, heating rope is flexible and occupies a small volume. It is also compatible with PID temperature controllers or computer control system such as Lab view control system. Therefore, the heating rope assisted method was chosen after considering its advantages at safety and easy control.

The heating zone is consists of three set of heating ropes and PID temperature controllers. The first heating rope and controller is in the preheat zone, which provides a rapid temperature ramp for the mixture from room temperature to 120°C. The second and third set of the heating components provide a constant heat source to maintain a flat, stable temperature profile. Because the feedback temperature control method is only good for a short length of tubing, two separate heaters are used to create two heating zones to extend the length of tubing that is heated. The total heat transfer was estimated

based on the temperature difference of the total volume of the fluid considering the fluid heat capacity. The length of the heating rope was estimated based on the total heat transfer plus an estimated heat loss rate and then divided by the unit length thermal input of the heating rope.

3.3 Condenser design

The heating unit is followed by a condenser, a counterclockwise single pass double tube heat exchanger, as the cooling zone. After the reaction mixture achieved a target residence time under the constant reaction temperature and pressure, the temperature of mixture solution was needed to cool down to room temperature. There are two main purposes of the cooling zone: the temperature must drop to stop or slow down the chemical reaction, and it must be low enough to keep the output solution under the saturation point which means to keep the outlet stream in liquid phase.

The length of the cooling zone and the diameter of the outside shell can be estimated from the heat transfer equation,

$$q_{tube} = UA\Delta T_{lm}$$

where q_{tube} is heat transfer into the tubing of the system, U is the total heat transfer coefficient, A is heat transfer area, and T_{lm} is log mean Temperature. The flow rate of the fluid, the physical properties of the fluid, the maximum reaction temperature, and the heat transfer coefficient for the material of the tubing are all known. The thickness and length of the tubing were estimated from the consideration of pressure range and

maximum reaction time. Therefore, the overall heat transfer coefficient can be estimated based on the equation,

$$\frac{1}{U} = \frac{1}{h_o} + \frac{t_w}{k_w} + \frac{1}{h_i}$$

Where h_o is the heat transfer coefficient of the outside fluid, h_i is the heat transfer coefficient of the inside fluid, t_w is the thickness of the wall, and k_w is the heat conductivity coefficient of the wall material. The inner tube of the heat exchanger is 1/8 inch OD and 0.085 inch ID of 304 stainless steel tubing and the outer tube is 3/8 inch OD 304 stainless steel tubing. The lab tap water was used as the cooling fluid which is introduced into the condenser. The minimum flow-rate of the cooling water can be calculated from the equation above as well, which is about 20mL/min.

3.4 Overall system

The continuous flow reaction system consists of two HPLC pumps (Chrom Tech Series III, P-2010), a heat rope with a temperature controller (Watlow), an inline filter, a Swagelok back pressure regulator, and 1/8 inch outside diameter stainless steel tubing, shown in **Figure.3.4**. Two precursor streams were simultaneously pumped into the flow reactor by two piston type HPLC pumps, mixed by a T-mixer, and then pass through a heating zone. The mixed solution gets heated up and maintains a high temperature at the heating zone and reaction zone, and get cooled down in the cooling zone. A backpressure regulator is applied to maintain a high system pressure after the cooling zone. The outlet stream from the backpressure regulator was collected. The

product particle was obtained from the outlet solution, which was centrifuged, washed with ethanol several times and dried under vacuum for two hours at room temperature.

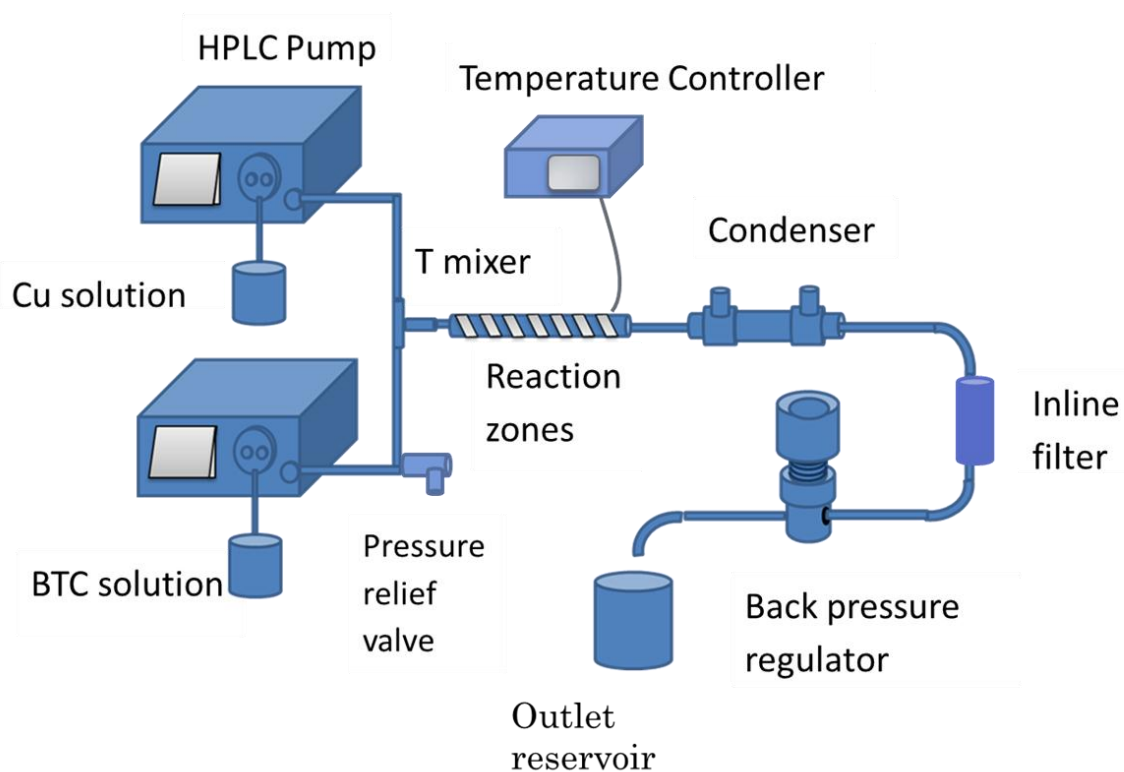


Figure 3.4 Schematic of first version of overall continuous flow reaction system design

3.5 First version of system

A simple system was designed initially to explore the challenges of this experiment.

This system helped to form better ideas for system improvement. Two major components were studied carefully: thermal energy transfer and liquid mixing

dynamics. A uniform heating profile of the mixture solution with easy control temperature steps are desired. The temperature range of the solution is from room temperature up to 250°C which is limited by the decomposition temperature of the MOF material determined by TGA result shown in **Appendix A**. For example, the heating zone of the first continuous system consists of a single heating rope with a PID temperature controller. Useful data was collected from the first experimental set-up to help to upgrade the heating performance. The heating zone depended on only one temperature measurement as the feedback signal. The temperature profile was expected to be non-uniform, which may be acceptable in the first design. Valuable information came from the system, which produced too much product crystal and after clogged the tubing of the system.

Another important component design is the solution mixing joint, the T mixer. The first mixing joint design used a 1/16 inch diameter stainless steel tee to mix the two different precursors. The simple tee allows the reactant fluid to pass through easily without clogging. A microchannel mixer is undesirable for this application because as the two precursors mix crystal growth occurs immediately, which could clog the microchannel in a fast growth study. After the growth rate study is done and ideal reaction conditions have been chosen, the mixer could be upgraded to a micro channel mixer to increase mixing capabilities.

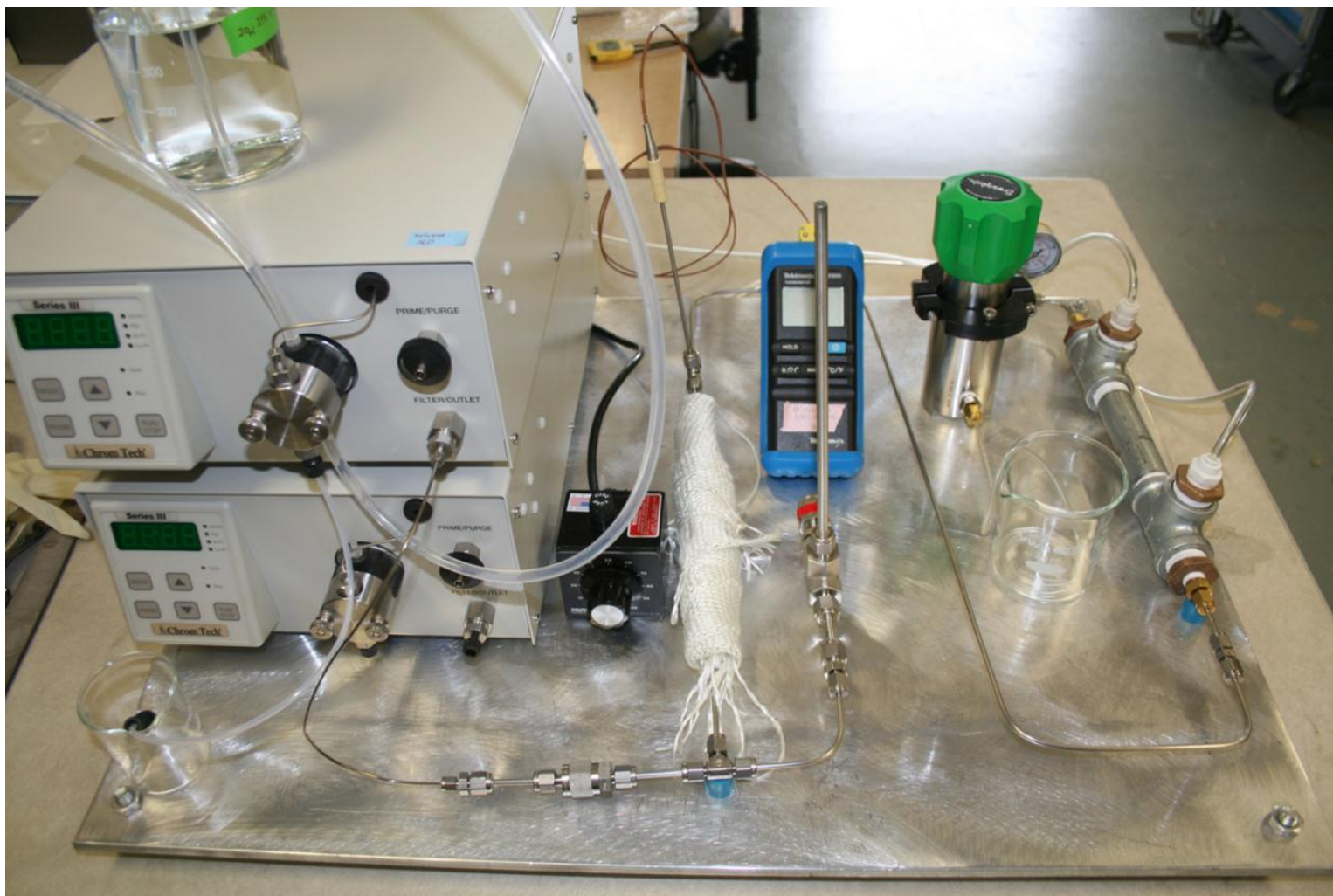


Figure 3.5 Picture of the first version of the synthesis system.

3.6 Experimental design

After setting up the first version of the continuous flow reactor system, upper and lower levels of the experimental parameters were determined. Reaction time, temperature, pressure, stoichiometry ratio, and solvent selection were the five main factors. By setting up the high and low levels of each factor and running all possible combinations, the most influential factor(s) are determined. There are total 25 experiment trials for the first system setup. An additional experiment plan will be made to explore the proper recipe based on the result of the first 25 trials.

Table 3.1 List of experiment parameters and their level

Factor	Low level	High Level
Reaction time	0.5 min	20.0 min
Temperature	60°C	250°C
Pressure	0 psig	3000 psig
Stoichiometry Ratio	Cu Rich	BTC Rich
Solvent ratio	100% water	100% EtOH

The initial system settings were based on the settings of the solvothermal batch reaction from our previous experiments. The order of magnitude of the upper level and lower level of each factor were based on results from the first system design. The reaction time is controlled by the precursor flow rate and the length of reaction zone. Adjusting the fluid flow from the HPLC pump is much easier than modifying the tubing length. Based on fixed length of the reaction zone of the first version reactor, the range of the

flow rate is from 0.5 mL/min to 10.0 mL/min. The reaction temperature can go up as high as 250°C based on the TGA result in Appendix A; Cu-BTC particles will be damaged above 300°C after losing all water contents. Considering the reaction temperature for the solvothermal batch reaction as 120°C, the expected reaction temperature will not go far from the successful temperature of the batch run. 250°C will be the highest temperature without affecting the product structure. System pressure is used to increase the boiling point of the reaction fluid. Over pressurizing the reactant would not affect the crystal growth by Arrhenius equation, but it will be good to check the crystal growth rate under an extremely high pressure. The stoichiometry ratio can cause large effects of the chemical reaction. Setting either Cu or BTC as the excess reactant would shift the reaction to a high yield of the limited product. Solvent selection is also important for crystal growth rate control as shown by a previous study[19]. Water is the solvent for copper nitrate and ethanol is the good solvent for trimesic acid. The water content in the copper nitrate solution can be substitute for ethanol from 0% to 100%.

Following the experimental plan, the drawbacks of the first version reactor system can be found. The tubing at the heating zone was clogged under the high reaction temperature due to non-uniform fluid temperature profile and crystal growth. The characteristic result of sample showed some difference from the reference in X-ray Diffraction and Raman spectroscopy which can help to adjust the recipe to achieve the expected products.

3.7 System upgrade version

Following the DoE method and after running several trials, some key components were upgraded, remodel, or even redesign based on the cycles of design of experiment: perform the experiment, collect the data, analysis and interpret the data, conclusion and decision, and modify and upgrade the system. Some key components had been upgraded or remodeled many time before the final system version. The heating zone was divided by three shorter feedback temperature control zones to have a better temperature profile. The heating zones are defined by the purpose of each: the first one is to preheat the mixture solution to a certain temperature, the second zone is to bring temperature to the reaction temperature, and the last one is to maintain the constant reaction temperature. The mixture solution was more uniformly heated from the upgrade design. The uniformity of the particle size from the product stream is getting better, as well. The micro channel mixer will be a good choice for this application to increase the mixing property. An economical way to increase the mixing property is to use a double screen-assisted inlet filter to generate a turbulent flow followed by the t-mixer. The solution will go through the mesh screen and get more thoroughly mixed before entering into the heating zone. The total length of the system is also reduced, especially the length between the condensing zone and stream outlet point. In the condensing zone, the temperature of the mixture is dropped down as much as possible to stop the reaction. The length after the condenser would be as short as possible to avoid buildup on the tubing wall.

Based on the consumption of the Cu, the yield of the Cu-BTC can be estimated about 97% from the outlet stream as the BTC rich condition.

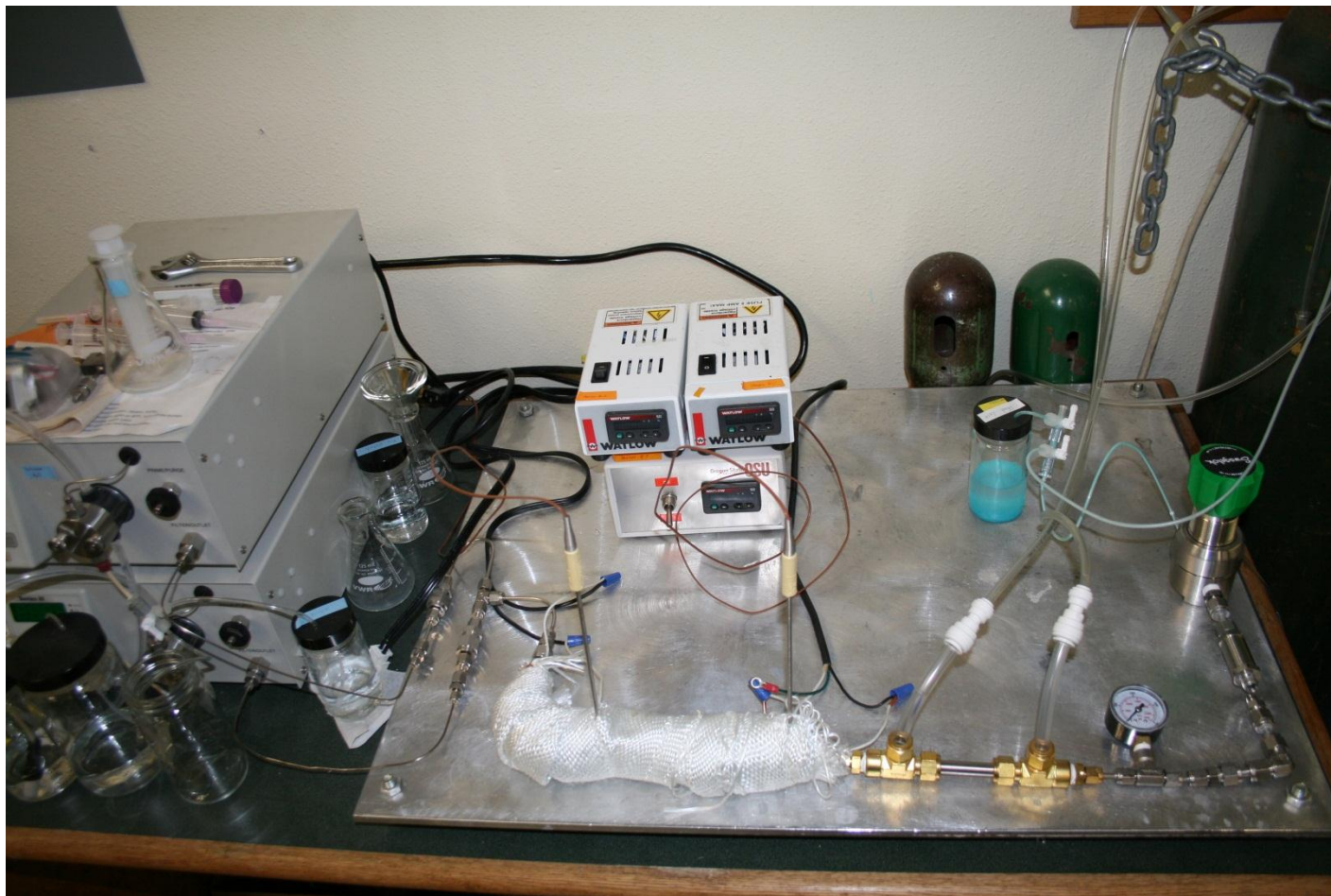


Figure 3.7 Picture of the upgraded version of the synthesis system.

Chapter 4

Results and discussion

The structural and morphological properties of Cu-BTC were characterized using XRD and SEM. Powder X-ray diffraction pattern was the first tool used to identify the crystal structure of the batch reaction product. A Bruker AXS D8-Discover X-ray diffractometer was used to obtain X-Ray diffraction (XRD) data under 40 mA and 40 keV. Scanning electron micrographs were obtained with Quanta 600F FEI SEM with an accelerating voltage of 5 keV. The XRD result from the continuous flow reactor matched the reference result from a solvothermal batch reaction and from the reference by Klimakow et al. [20]

4.1 X-ray Diffraction (XRD)

The interference patterns of X-ray scattering by crystals is explained by Bragg's law which is an important tool to identify the crystal structure for comparing two different synthesis methods. The XRD result of the solvothermal synthesis method can be used as the reference to compare with the result from the continuous method as shown in **Figure 4.1**. All the corresponding peaks were identical on 2θ between the continuous reaction and batch reaction even though the intensities of the corresponding peak are different due to the average crystal size discrepancy. From the Scherrer equation, the average crystal size is related to the full width at half maximum.

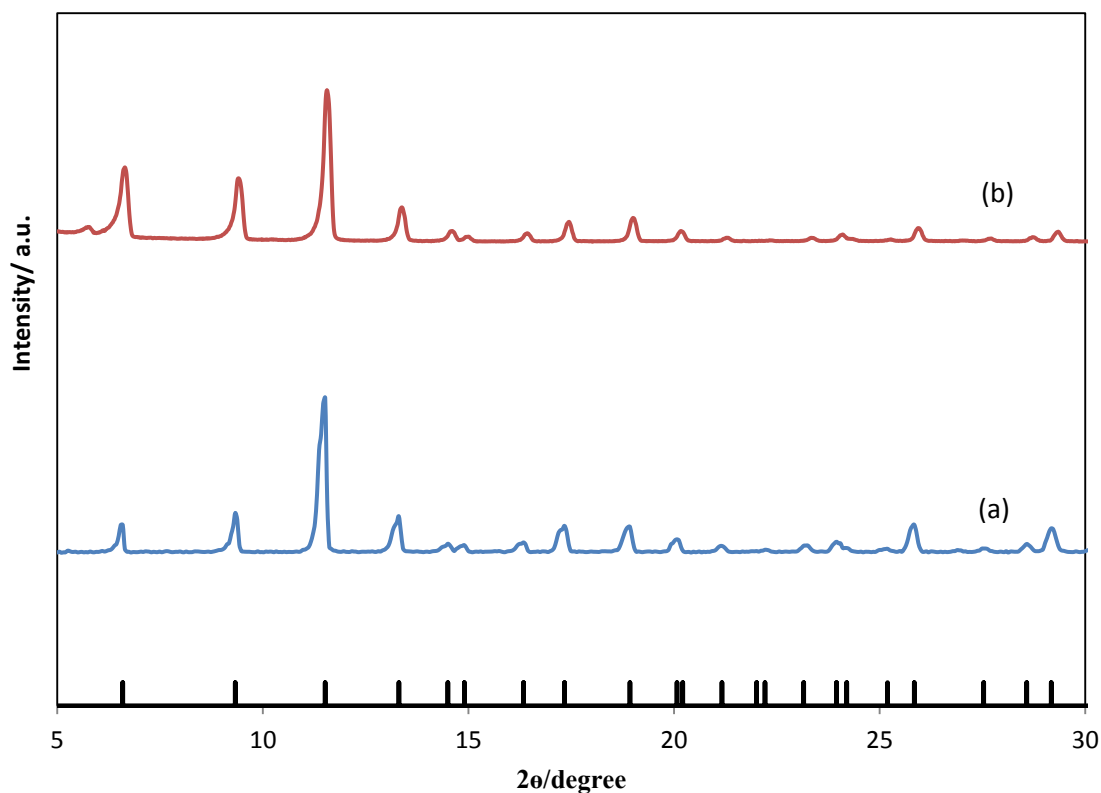


Figure 4.1 XRD patterns of Cu-BTC samples of (a) batch reaction method and (b) continuous reaction method. Reflections for Cu-BTC calculated from the crystal structure are given for comparison.[20, 21]

4.2 Raman Spectroscopy result

Since the metal-organic framework (MOF) material contains organic linkers, chemical bonding and symmetry of the molecule can be identified through the vibration of the compound using Raman Spectroscopy. The results of the Raman spectra are dominated by the organic bonding of the MOF framework, such as C-C, C=C, C-H, and more.

Raman bands were found at 1611 and 1004, which correspond to the $\nu(\text{C}=\text{C})$ modes of the benzene ring; the bands at 824 and 742 cm^{-1} correspond to out-of-plane ring (C-H) bending vibrations and to out-of-plane ring bending. The bands at 1540 and 1460 cm^{-1} are due to the $\nu_{\text{asym}}(\text{C}-\text{O}_2)$ and $\nu_{\text{sym}}(\text{C}-\text{O}_2)$ stretching modes. The band at 500 cm^{-1} is associated (Cu-Cu) modes in the low-frequency region (600-170 cm^{-1} range). [20]

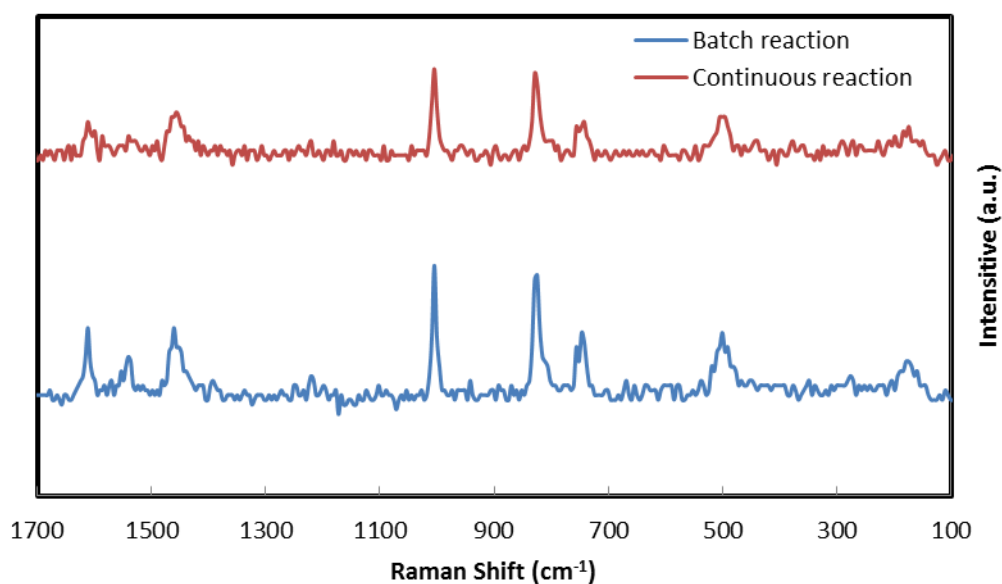


Figure 4.2 Raman Spectra of batch and continuous reaction samples.

4.3 SEM image

The morphology of the MOF crystal can be studied in more depth by taking SEM images. The range of the crystal size of fully crystallized Cu-BTC at different reaction temperature is from 200 nm up to 20 μm , which is a good scale range for the SEM. A high conductivity sample is required for SEM detection to avoid extra electron charge

accumulated on the surface of the scanning sample. A thin nano-scale gold/palladium layer was coated on the top of the Cu-BTC sample to increase its electrical conductivity; this coating enhanced the image resolution to achieve a magnification of around 50000x. In addition, reducing the electron voltage and the spot size helped to reduce the exceeded free electrons. For the same reason, using a slice of silicon wafer or aluminium sheet as the sample substrate would be better than glass based on the higher conductivity of these substrates.

The shapes of the Cu-BTC crystals are octahedron from the observation of SEM image for both batch and continuous reaction. The size distribution is varying. The average size of the crystal would be about 10 μ m to 20 μ m, though crystals can range from 100nm to 30 μ m. The morphology result from SEM for the continuous flow reaction product is very similar to that of the batch reaction. However, the size distribution of the crystals formed in the continuous process was in a smaller range from 50nm to 500nm.

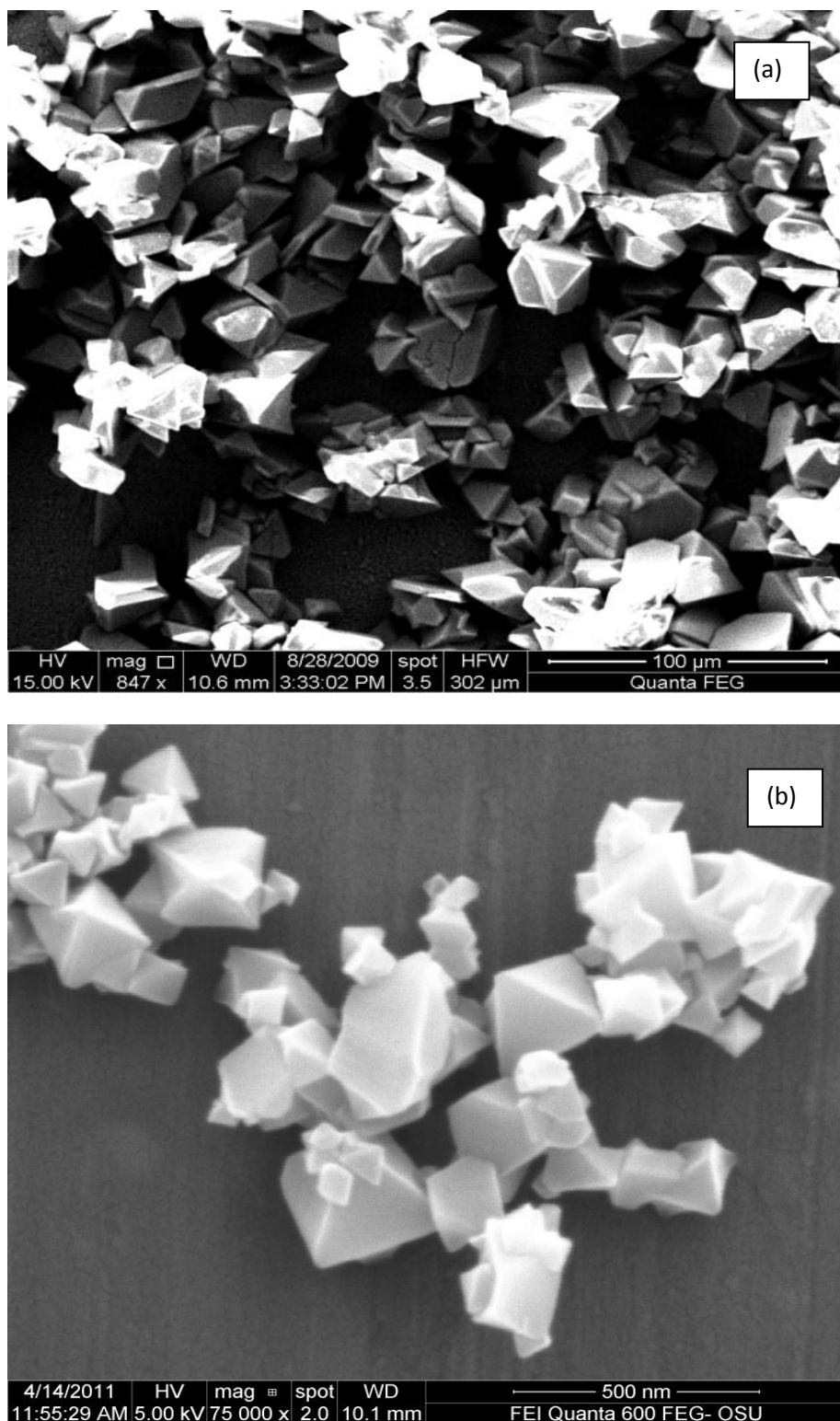


Figure 4.3 SEM image of Cu-BTC samples of (a) Solvothermal batch reaction (b) continuous reaction.

4.4 Water effect

The average Cu-BTC crystal size could be control from micron-size to nano-size by adjusting the water/ethanol ratio in the $\text{Cu}(\text{NO}_3)_2$ solvent, see **Figure 4.4**. The presence of water in the precursor solution significantly influenced both nucleation rate and crystallization rate. The nucleation rate in the water-free solvent is much larger than in the water/ethanol solvent, which caused more small particles to form. As the tradeoff, the crystallization rate in water/ethanol solvent was greater than the particle formed in water free solvent. Cu ions and BTC ions were initially surrounded by water/ethanol ions and BTC ions were tempting to replace water/ethanol ions. Organic ligands more readily replaced ethanol ions than water ions and then they connected to Cu ions to form a metal-organic network. Therefore, nucleation was increased in the ethanol solvent compared to one with water present. On the other hand, the Cu-BTC product would be shifted to an uncompleted network structure if the water composition is unrestricted. Water molecules would bond to the Cu ion and occupy a connection instead of BTC ion. An XRD result confirms that a byproduct increases when the water ratio exceeds the appropriate level. In addition to the size control, controlling the nucleation and crystallization from solvent selection has a greater effect on crystal growth than to adjust the reaction residence time and reaction temperature. Using the water/ethanol solvent would have a smaller production rate than in a pure ethanol solution since it has a lower nucleation rate but crystal growth is much fast.

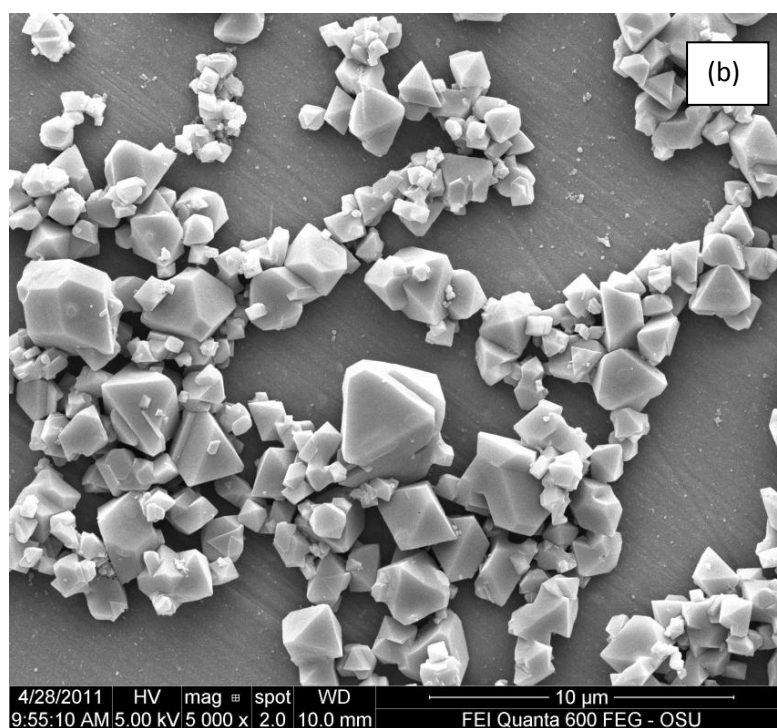
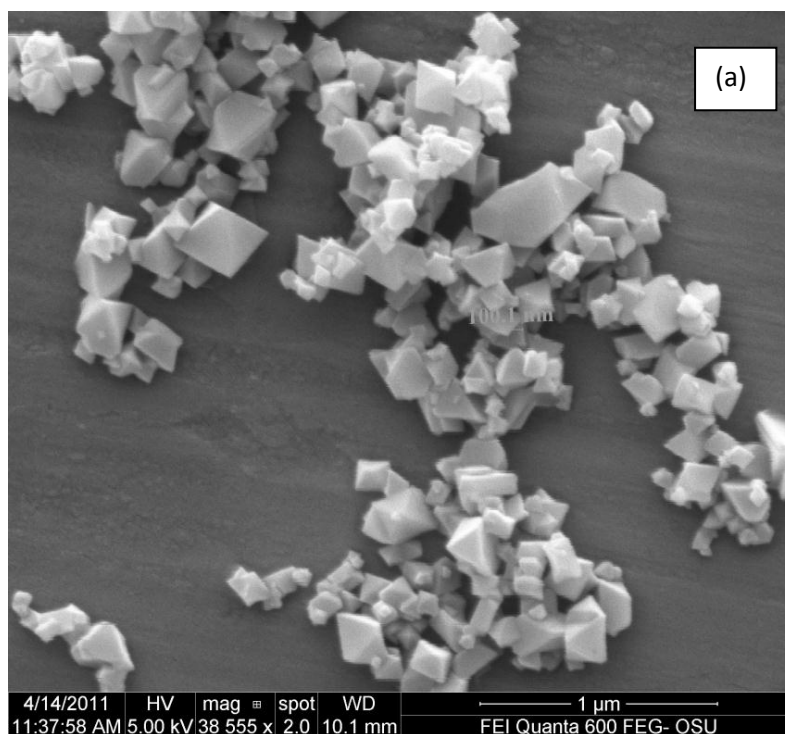
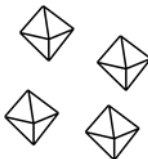



Figure 4.4 SEM image of Cu-BTC sample of (a) continuous reaction, (b) batch reaction.

There are two common situations in MOF growth: crystallization-dominated growth and nucleation-dominated growth. When the nucleation growth rate is rapid the solution contains a high number of smaller crystals. The heterogeneous reaction in this case occurs quickly with the seed nucleus forming a new crystal. For the nucleation-dominated growth, a large number of small crystals would be formed rather than a small number of large crystals. On the other hand, less nucleation growth and larger crystal size results from a crystallization growth rate dominated situation.

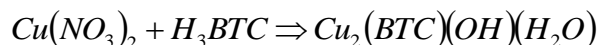
Table 4.1 Crystal growth at same reaction temperature, flow rate, pressure, and reactant ratio.

	Reaction time	Solvent	Crystal size / quantity
Crystallization dominated	Slow	Ethanol/Water	
Nucleation dominated	Quick	Ethanol only	

4.5 Stoichiometry ratio effect

The chemical reaction rate is dependent on the stoichiometry ratio of the reactants. The chemical reaction is affected and under a different reaction route upon changing the reactant ratios. A similar structure $Cu_2(BTC)(OH)(H_2O)$ can be achieved with a copper rich reaction.





H_3BTC ions were dissolved in water as the precursor. H_3BTC molecules were surrounded by the water molecules. Cu-BTC product is not easily formed since water molecules bind to the BTC ions under certain reaction conditions depending on temperature, flow rate, and mole ratios. In a Cu ion rich condition, the final product would be $Cu_2(BTC)(OH)(H_2O)$ instead of $Cu_3(BTC)_2$. According from the experiment, the by-product $Cu_2(BTC)(OH)(H_2O)$ could be produced from the original recipe under a high temperature with high Cu ion ratio. The XRD result from different stoichiometry ratio shows that two different products can be produced using the same reactants under different reaction condition, shown in **Figure 4.5**. An interesting question was raised regarding the by-product: does the by-product come from a reaction intermediate or from the product? The by-product is not only formed from the original reaction but also can be formed directly from the product. It can be obtained from the product in an excess water environment under a high temperature or after a long period of time. My result shows that the Cu-BTC product was placed into a water environment; it would decompose into the by-product after one week. It approved that the product of $Cu_3(BTC)_2$ would also react with water to form $Cu_2(BTC)(OH)(H_2O)$. In other words, the Cu-BTC is stabilized in ethanol or an ethanol/water mixture rather than in an aqueous solution. The color of the particle was observed to change from dark blue to light blue when the Cu-BTC product expose to the aqueous solution.

According from the previous study, by-product appearance is influenced by the presence of water. By adjusting the reactant ratio to be BTC-rich, the composition in

the outlet stream was changed from the by-product only to by-product mixing with product according to the XRD result in **Figure 4.5**. A complicated XRD spectrum is shown, which represents more than one major chemical in the final mixture. By comparing with a reference XRD spectrum from the batch reaction, by-product and product can be identified.

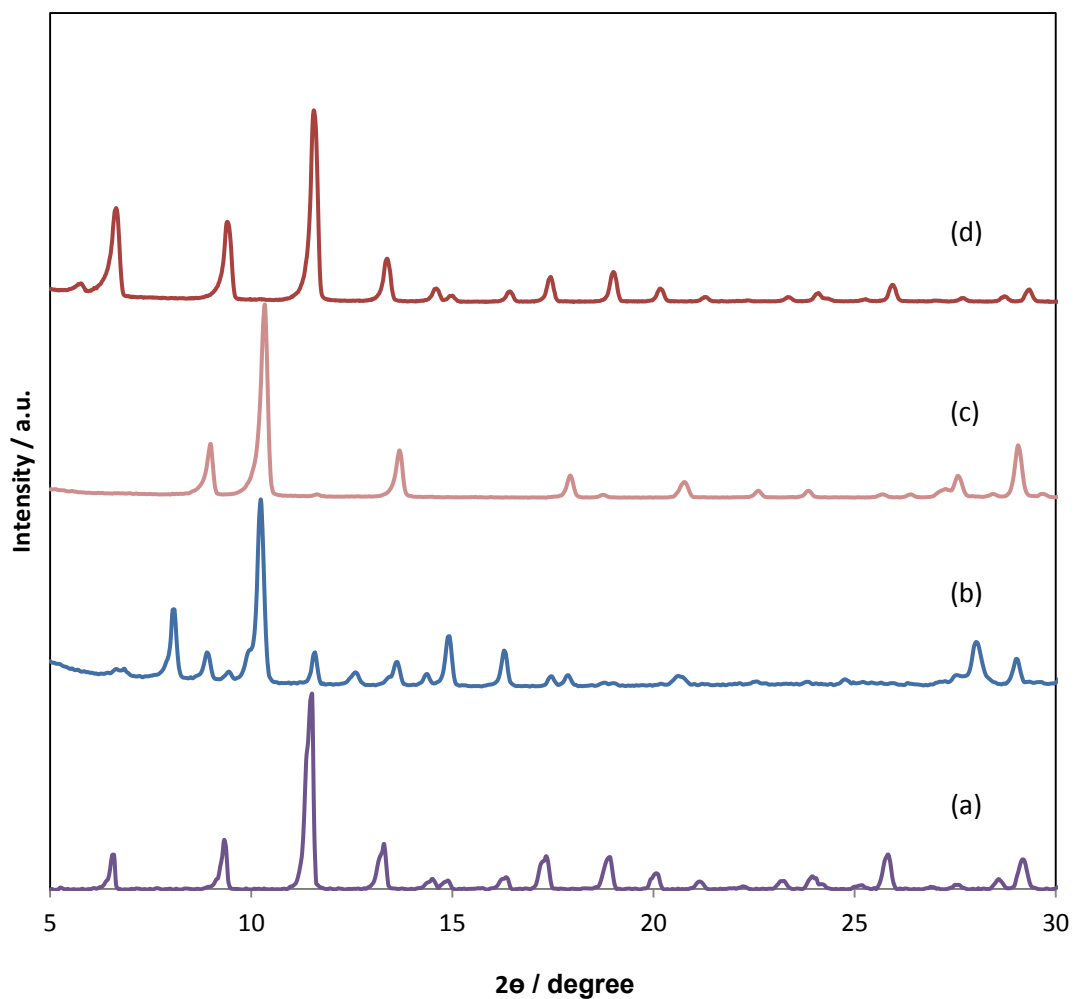


Figure 4.5 XRD results of Cu-BTC crystal from (a) batch reaction, and from continuous flow reaction with Cu:BTC ratio in (b) 1:1, (c) 2:1, and (d) 1:3.

4.6 Temperature effect

Besides the solvent selection, crystal growth was also impacted by the different reaction temperatures due to the reaction kinetic theory.[22] The reaction rate constant depends on reaction temperature based on the Arrhenius equation. The system temperature also contributed to speed up the crystallization growth rate, which affects the size of the crystal. A study was performed to investigate the crystal size under different reaction temperatures. As a convenient feature of the flow reactor system, the reaction temperature can be easily adjusted from 25 °C to 180 °C and the reactant is ensured to be in liquid phase by the increased system pressure. The system pressure is set 1000psi to ensure all reactants are liquid phase and the reaction occurs as homogeneous. Varying the system pressure above mixture boiling point does not affect the crystal growth. The Cu-BTC crystals are grown with an increased reaction temperature; **Figure 4.6** shows that the crystal average diameter can be grown up to about 250nm in 100°C and about 100 nm in 65 °C.

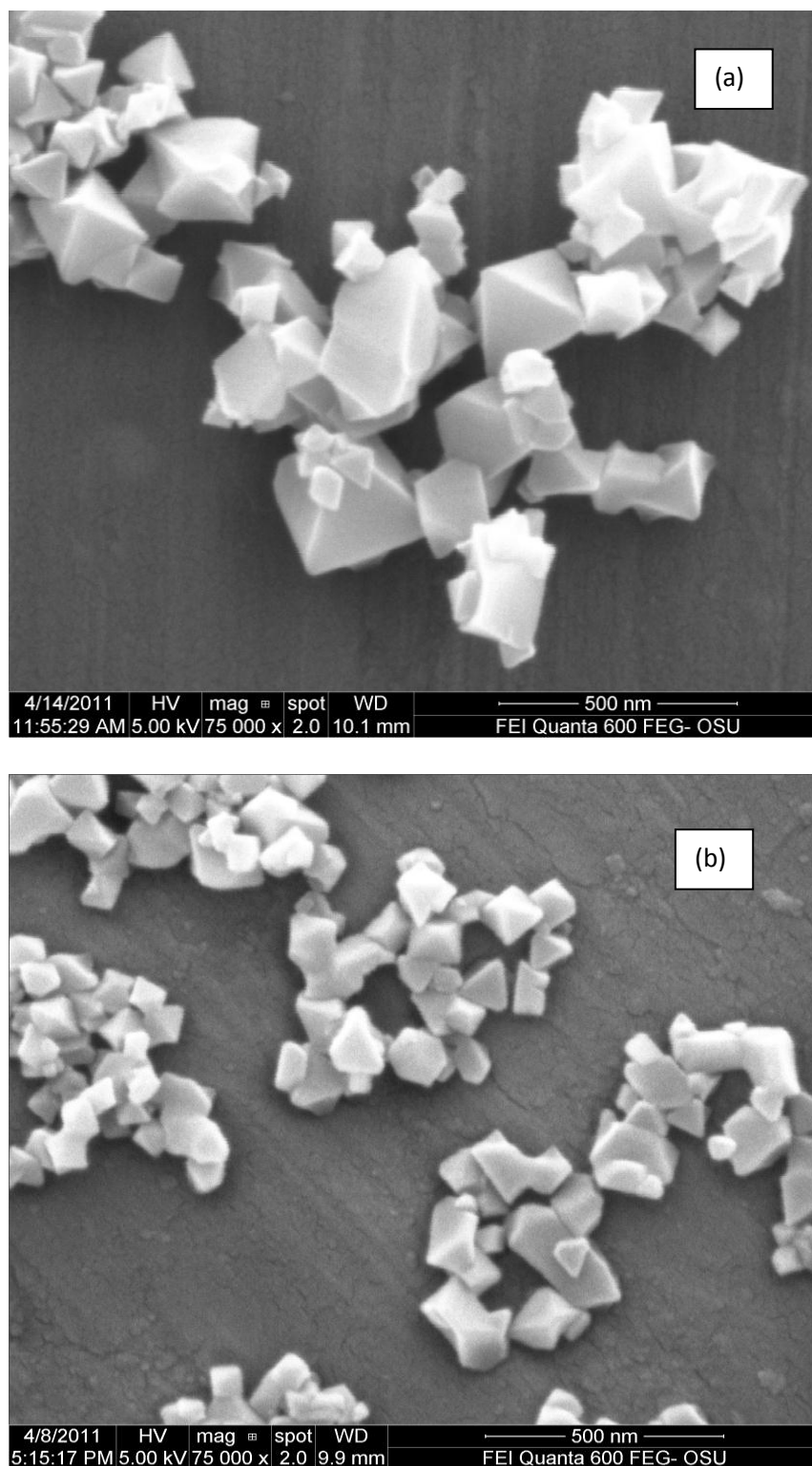


Figure 4.6 SEM image of Cu-BTC with synthesis temperature at (a) 120 °C, (b) 65 °C.

4.7 Film deposition

MOF crystal can grow on different substrates under a solvothermal condition, which was observed in a batch process in a closed pressurized chamber.[23] The applications of the MOF material are most likely focused on gas adsorption. A dense film of the MOF crystal coating on a specific surface would be most applicable for these applications. Therefore, MOF crystal growth on a substrate with a rapid process method is desired in the current research.

A thermal-assisted crystal grow process is introduced following the continuous flow reaction system shown in **Figure 4.7.1**. The production stream comes out from the back pressure regulator of the continuous flow reactor and then is introduced to an apparatus that contains a hotplate to heat up a substrate. The operation temperature is chosen between 100 °C to 250°C, depending on the desired crystal size. Cu-BTC crystals were deposited on an Al₂O₃ substrate as shown in Figure 4.7.1. Crystals did not cover the substrate surface very well, possibly due to the deposition conditions such as temperature and surface treatment. A microreactor-assisted nano deposition (MAND) system will be a good candidate to coat a dense uniform Cu-BTC film on a designed substrate since it will have great solution mixing and uniform particle deposition. A heterogeneous reaction between solution and surface of the deposited substrate will be expected to occur to allow the Cu-BTC crystals to grow on the substrate. In future work a heating unit coupled with a spin coater will be used to speed up the reaction and to achieve a better deposited uniformity.

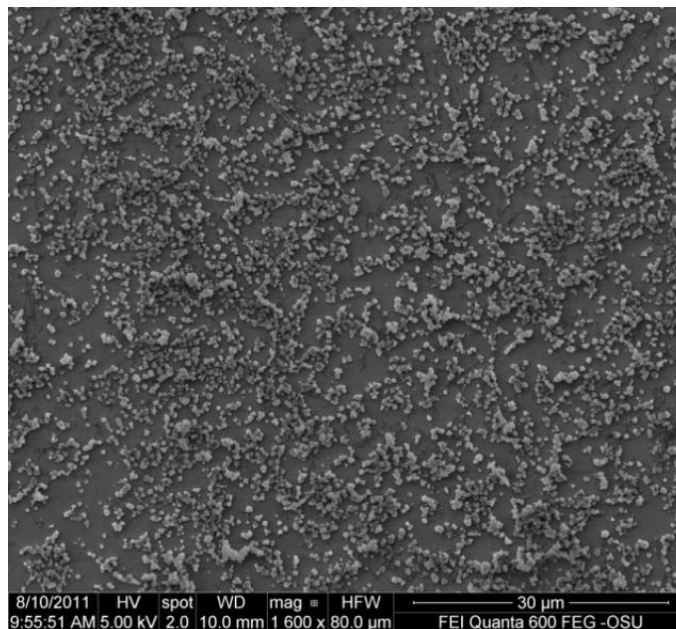


Figure 4.7.1 SEM image of Cu-BTC with synthesis temperature at 65 °C

Since the carboxylic group carries a weak negative charge, Cu-BTC crystals can also be deposited on a substrate with a positively charged layer, like polyelectrolyte multilayers (PEMs).[24] Positively charged poly (allylamine hydrochloride) (PAH, 15000 g/mol) and negatively charged poly (sodium 4-styrene sulfonate) (PSS, 70000g/mol) are deposited alternatively on the glass substrate as a charged layer. The PAH will be the last layer on the top of the surface. The number of the PAH/PSS layers affected the adsorption of the Cu-BTC crystal, shown in **Figure 4.7.2**. A Cu-BTC deposition on 7 charged layers PAH/PSS was denser than on 5 layers.

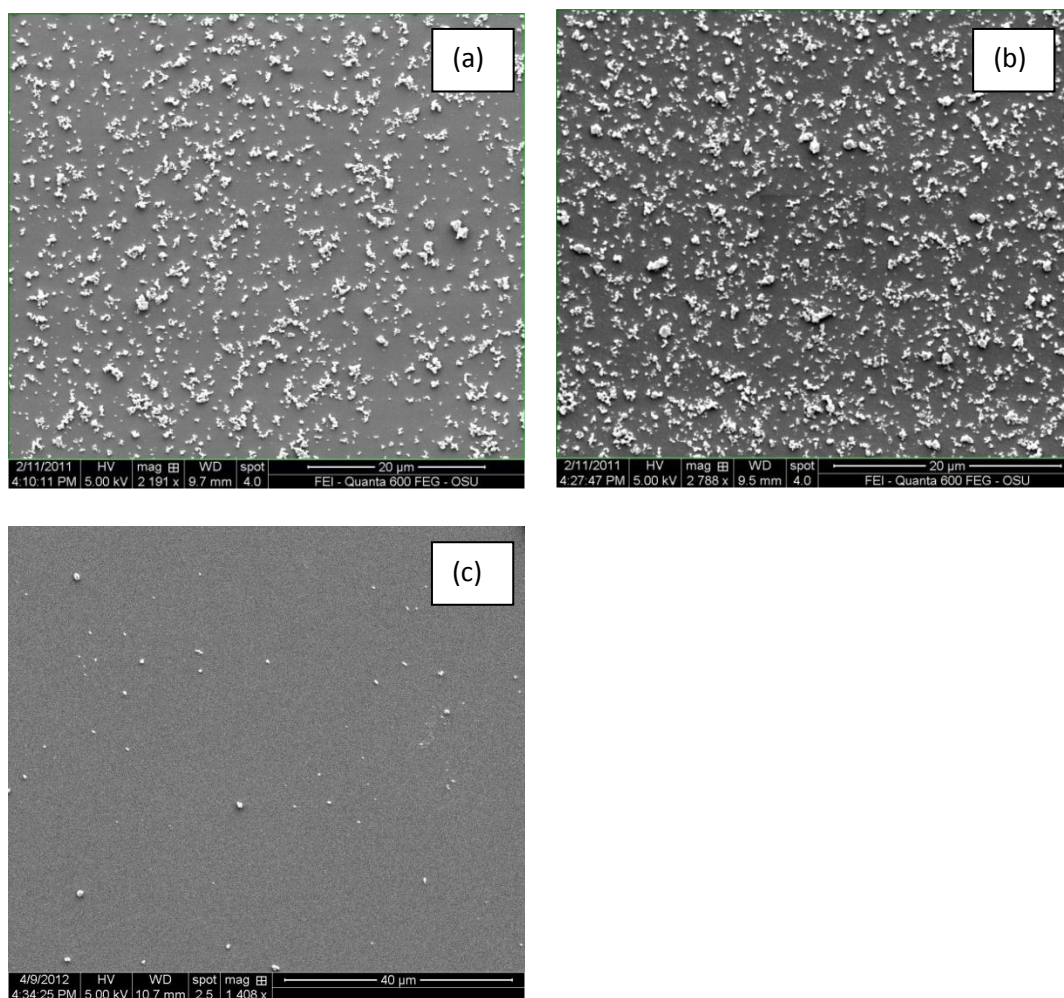


Figure 4.7.2 SEM image of Cu-BTC deposited on the top of (a) (PAH/PSS) n PAH layer at $n=5$, (b) (PAH/PSS) n PAH layer $n=7$, and (c) (PAH/PSS) n layer at $n=5$.

Chapter 5

Conclusion and Future work

The continuous synthesis method provides a new rapid way to produce a nano-size bulk Cu-BTC particle, a common metal-organic framework (MOF) material. The crystallization is easy to control by changing the reaction conditions such as residence time, reaction temperature, solvent composition, and precursor concentration. Therefore, the crystal size can be controlled to achieve a better size uniformity. Our study also confirms that while the system pressure does not have a significant influence on the crystal growth, a high pressure condition is needed to maintain a liquid phase above the solvent evaporation temperature. Solvent composition and reaction temperature were two of the most important control factors for size growth. They affect the crystallization and nucleation rates in the crystal growth mechanism. The final product requires a simple separation process since the final product is in the ethyl alcohol/water solution, which can be recycled to be more environmentally friendly. The reaction time is only required 10 to 20 minutes compared to 18 hours using a batch synthesis method, like a solvothermal reaction method. The average crystal size of Cu-BTC from the batch reaction is 20 microns. From the continuous flow reaction, the average size of Cu-BTC crystals was reduced to 50 to 100 nanometers, which is ideal for applications that need nanoscale crystals, such as microsensors. The new method provides not only to obtain a high production yield as 97% but also a high efficiency to synthesize the metal- organic framework particles.

The continuous reaction system can be further scaled up by increasing the volumetric flow rate with larger tubing or by adding parallel system reaction units. This study use Cu-BTC crystals, a Cu ion connected to a BTC organic linker, as the example MOF material. It will be also applicable to all other MOF materials with a structure of metal ions connected to organic linkers, based on the similar framework connection and physical properties.

Film deposition is the most common way to apply nanoscale MOF crystals. We have explored film deposition using product solution from continuous flow reactors. The current study shows that the surface charge property affects the uniformity of the deposition film. There are still challenges to synthesize a thin, condense MOF film using this method. A possible method will be using a thermal spin coating apparatus in combination with the continuous flow reactor to make a film deposition, like microreactor-assisted nano deposition (MAND) system. It will be the future work of this project. It also will be a challenge to reduce the crystal size less than 50nm.

Bibliography

1. Schlapbach, L. and A. Züttel, *Hydrogen-storage materials for mobile applications*. Nature, 2001. **414**(6861): p. 353-358.
2. Rosi, N.L., et al., *Hydrogen storage in microporous metal-organic frameworks*. Science, 2003. **300**(5622): p. 1127-1129.
3. Lee, J., et al., *Metal-organic framework materials as catalysts*. Chemical Society Reviews, 2009. **38**(5): p. 1450-1459.
4. Li, J.R., R.J. Kuppler, and H.C. Zhou, *Selective gas adsorption and separation in metal-organic frameworks*. Chemical Society Reviews, 2009. **38**(5): p. 1477-1504.
5. Tomic, E.A., *THERMAL STABILITY OF COORDINATION POLYMERS*. Journal of Applied Polymer Science, 1965. **9**(11): p. 3745-&.
6. Li, H., et al., *Design and synthesis of an exceptionally stable and highly porous metal-organic framework*. Nature, 1999. **402**(6759): p. 276-279.
7. Kuc, A., A. Enyashin, and G. Seifert, *Metal-organic frameworks: Structural, energetic, electronic, and mechanical properties*. Journal of Physical Chemistry B, 2007. **111**(28): p. 8179-8186.
8. Eddaoudi, M., et al., *Systematic design of pore size and functionality in isorecticular MOFs and their application in methane storage*. Science, 2002. **295**(5554): p. 469-472.
9. Shekhah, O., et al., *MOF thin films: existing and future applications*. Chemical Society Reviews, 2011. **40**(2): p. 1081-1106.
10. Millange, F., et al., *A time-resolved diffraction study of a window of stability in the synthesis of a copper carboxylate metal-organic framework*. Crystengcomm, 2011. **13**(1): p. 103-108.
11. Schlesinger, M., et al., *Evaluation of synthetic methods for microporous metal-organic frameworks exemplified by the competitive formation of Cu(2)(btc)(3)(H(2)O)(3) and Cu(2)(btc)(OH)(H(2)O)*. Microporous and Mesoporous Materials, 2010. **132**(1-2): p. 121-127.
12. Gassensmith, J.J., et al., *Microcontact Click Printing for Templating Ultrathin Films of Metal-Organic Frameworks*. Langmuir, 2011. **27**(4): p. 1341-1345.
13. Zhao, Z.X., et al., *Synthesis, characterization and gas transport properties of MOF-5 membranes*. Journal of Membrane Science, 2011. **382**(1-2): p. 82-90.
14. Yang, Q., et al., *Molecular simulation of separation of CO₂ from flue gases in Cu-BTC metal-organic framework*. Aiche Journal, 2007. **53**(11): p. 2832-2840.
15. Zacher, D., et al., *Thin films of metal-organic frameworks*. Chemical Society Reviews, 2009. **38**(5): p. 1418-1429.
16. Yoo, Y. and H.-K. Jeong, *Rapid fabrication of metal organic framework thin films using microwave-induced thermal deposition*. Chemical Communications, 2008(21): p. 2441-2443.
17. Yuan, W., et al., *Study of the mechanochemical formation and resulting properties of an archetypal MOF: Cu(3)(BTC)(2) (BTC=1,3,5-benzenetricarboxylate)*. Crystengcomm, 2010. **12**(12): p. 4063-4065.
18. Shekhah, O., et al., *Layer-by-layer growth of oriented metal organic polymers on a functionalized organic surface*. Langmuir, 2007. **23**(14): p. 7440-7442.
19. Rosi, N.L., et al., *Advances in the chemistry of metal-organic frameworks*. Crystengcomm, 2002: p. 401-404.

20. Klimakow, M., et al., *Mechanochemical Synthesis of Metal-Organic Frameworks: A Fast and Facile Approach toward Quantitative Yields and High Specific Surface Areas*. Chemistry of Materials, 2010. **22**(18): p. 5216-5221.
21. Chui, S.S.Y., et al., *A chemically functionalizable nanoporous material Cu-3(TMA)(2)(H2O)(3) (n)*. Science, 1999. **283**(5405): p. 1148-1150.
22. Kleist, W., M. Maciejewski, and A. Baiker, *MOF-5 based mixed-linker metal-organic frameworks: Synthesis, thermal stability and catalytic application*. Thermochemica Acta, 2010. **499**(1-2): p. 71-78.
23. Zacher, D., et al., *Deposition of microcrystalline Cu-3(btc)(2) and Zn-2(bdc)(2)(dabco) at alumina and silica surfaces modified with patterned self assembled organic monolayers: evidence of surface selective and oriented growth*. Journal of Materials Chemistry, 2007. **17**(27): p. 2785-2792.
24. Wang, W., et al., *Self-Assembly of Nanostructured Diatom Microshells into Patterned Arrays Assisted by Polyelectrolyte Multilayer Deposition and Inkjet Printing*. Journal of the American Chemical Society, 2009. **131**(12): p. 4178-+.

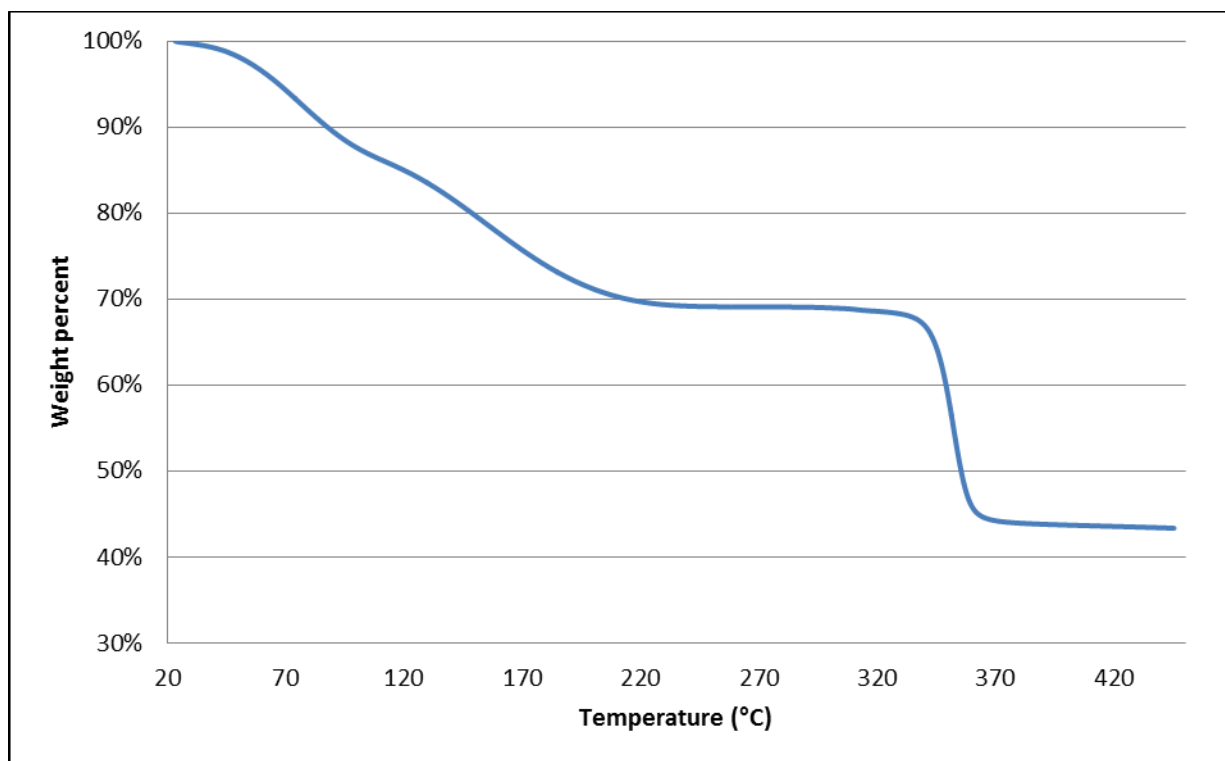
Appendix A

Figure App. Cu-BTC TGA result of solvothermal batch reaction.